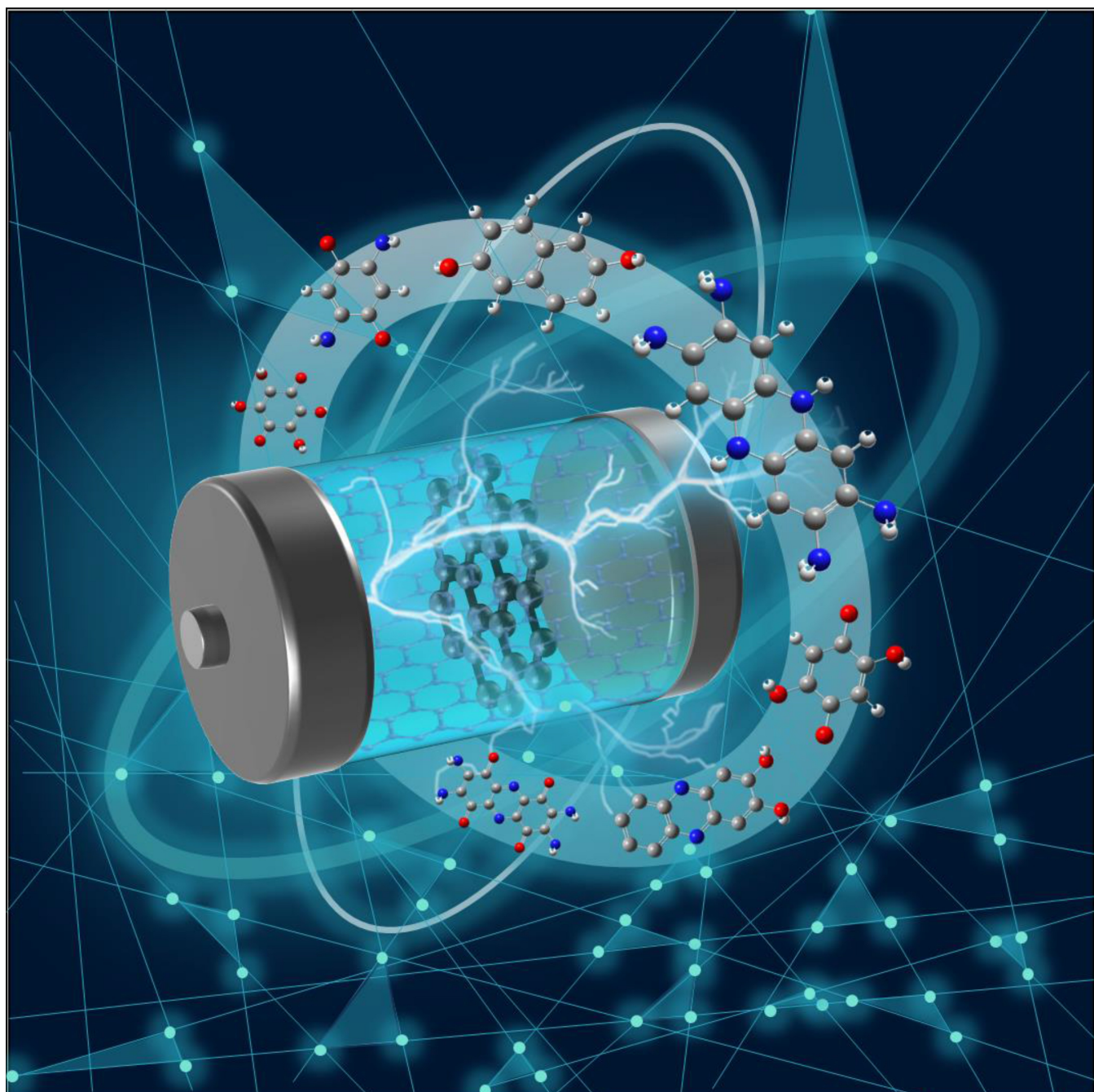


A Review on the Role of Hydrogen Bonds in Organic Electrode Materials

Yonghui Wang,^[a] Yuxuan Zhao,^[a] Xinlei Xu,^[a] Weizhe Gao,^[a] Qichun Zhang,^{*[b, c]} and Weiwei Huang^{*[a]}



Organic electrode materials (OEMs) hold significant development potential in the field of batteries and are regarded as excellent complementary materials to resource-limited inorganic electrode materials, which have recently been the subject of extensive research. As research deepens, an increasing number of scholars recognize the influence of weak bond interactions on the properties of OEMs. Generally, weak bond interactions have more pronounced effects on organic materials compared to inorganic ones. Among various weak interactions, hydrogen bonds are particularly noteworthy, having been

proven to play crucial roles in adjusting electrode charge distribution, stabilizing crystal structures, and inhibiting cyclic dissolution. The studies of hydrogen bonds in OEMs are therefore of paramount importance for guiding their future development. In this review, we primarily summarize the research progress in hydrogen bond science within OEMs and discuss future research directions and development prospects in this area. Hoping to provide valuable references for the advancement of OEMs.

1. Introduction

Organic electrode materials (OEMs) possess significant advantages, including high theoretical specific capacity, customizable structure, and environmentally friendly characteristics. Under some circumstances, they might take the place of inorganic electrode materials in energy storage applications. However, the development of OEMs has not been smooth sailing. Since the late 1960s, when the N-chloro compound dichloroisocyanuric acid (DCA)^[1] was reported for use in lithium-ion batteries (LIBs), a variety of organic materials, for example, quinone,^[2] pyromellitic dianhydride (PDA),^[3] and polyaniline (PAn),^[4] have been investigated as electrode materials. However, the discovery that inorganic transition metal complexes can reversibly store Li⁺ at high potentials and capacities led to declines in the research focus on OEMs. In recent years, driven by the soaring demand for batteries and the limited resources of inorganic electrode materials, high-performance, low-cost, and abundantly available OEMs have garnered increasing attention from researchers, and significant progress has been made, with numerous new structural organic materials being reported. To date, the reported OEMs incorporate yet are not restricted to, carbonyl compounds,^[5] conductive polymers,^[6] azo compounds,^[7] imine compounds,^[8] and metal-organic complexes.^[9] With the continued research into OEMs, the role of weak bond interactions in battery cycling has become increasingly recognized by scholars. For the most part, light components like C, H, N, and O make up OEMs. Beyond the carbon skeleton, these materials are abundant in active groups containing strongly electronegative elements (e.g., C=N, N=N, C=O). The presence of numerous strongly electronegative elements renders OEMs excellent hydrogen bond acceptors (HBAs). In the presence of appropriate hydrogen bond donors

(HBDs), there is potential for forming hydrogen bond networks through weak interactions, which can significantly influence the batteries' performance.

The concept of hydrogen bonds was first articulated in 1920 by Latimer and Rodebush when discussing polarity and ionization according to the viewpoint of the Lewis hypothesis of valence.^[10] At that time, the concept was highly controversial, with many scientists questioning how a hydrogen atom could participate in two "covalent bonds". The works of Huggins and Pauling were pivotal in consolidating and popularizing the concept of hydrogen bonds. In 1936, Huggins^[11] first explained the rapid movement of hydrogen ions in water by "proton transition", further developing the Grothuss proton transport mechanism. Pauling's book of 1939, "The Nature of the Chemical Bond",^[12] formalized the concept of hydrogen bonds, significantly advancing chemical science. After years of research, IUPAC^[13] updated the definition of hydrogen bonds in 2011: "The hydrogen bond is an attractive interaction between a hydrogen atom from a molecule or a molecular fragment X-H, in which X is more electronegative than H, and an atom or a group of atoms in the same or a different molecule, in which there is evidence of bond formation." This definition is now widely accepted in chemistry. The hydrogen bonds typically consist of HBDs (X) and HBAs (Y), denoted by the general formula X-H...Y. Classical hydrogen bonds consider X and Y to be atoms with little radii and high electronegativity, like F, O, and N, with Y having at least one solitary sets of electrons.^[14] However, the scope of hydrogen bonds has expanded with further study(Figure 1a). π bonds or transition metal atoms have been found to act as HBAs to form non-classical hydrogen bonds, such as C-H...Y interactions,^[15] π-type hydrogen bonds formed by X-H...π interactions,^[16] and dihydrogen bonds formed by X-H...H-M interactions.^[17] Compared to classical strong hydrogen bonds, non-classical hydrogen bonds play limited roles in electrode materials. Therefore, this review focuses on the influence of representative classical hydrogen bonds on the properties of OEMs.

Based on binding energy, bond angle, and bond length, Taylor and Jacobsen^[18] divided different kinds of hydrogen bonds into three categories: strong, moderate, and weak hydrogen bonds. This classification also serves as a criterion for determining the presence of hydrogen bonds in the battery system. Within the battery system, the electrode materials can form intramolecular hydrogen bonds (Intra-HBs) between the HBDs and the strongly electronegative active group atom,^[19]

[a] Y. Wang, Y. Zhao, X. Xu, W. Gao, W. Huang
School of Environmental and Chemical Engineering, Yanshan University,
Qinhuangdao 066004, China
E-mail: huangweiwei@ysu.edu.cn

[b] Q. Zhang
Department of Materials Science and Engineering, City University of Hong Kong, Hong Kong SAR 999077, P. R. China
E-mail: qizhang@cityu.edu.hk

[c] Q. Zhang
Center of Super-Diamond and Advanced Films (COSDAF), City University of Hong Kong, Hong Kong SAR 999077, P. R. China
E-mail: qizhang@cityu.edu.hk

intermolecular hydrogen bonds (Inter-HBs) between material molecules,^[20] Inter-HBs between the materials and the binders,^[21] and Inter-HBs between the material and the electrolytes.^[22] It can be said that hydrogen bonds play crucial roles throughout the batteries' operation and significantly impact their performance.

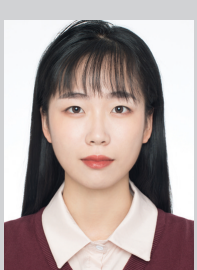
With the rapid advancement of OEMs in recent years (Figure 1b), increasing studies have focused on the role of hydrogen bonds in these materials, necessitating a summary of the key findings in this area. This review introduces the research progress on the Intra-HBs and Inter-HBs in OEMs, classified by different HBDs ($-\text{OH}$, $-\text{NH}-$, $-\text{NH}_2$). Additionally, it proposes future directions for research and development in hydrogen bond science within OEMs. Hoping to provide valuable insights for the advancement of OEMs.



Yonghui Wang obtained his B.S. degree of applied chemistry at Yanshan University in 2022. Now, he is a Master's candidate in Prof. Weiwei Huang's group at Yanshan University. His research focuses on the synthesis and fabrication of organic cathode materials for Zn batteries.



Yuxuan Zhao received her B.S. in applied chemistry from Hebei University of Engineering in 2022. She is currently pursuing her Master's degree in Prof. Weiwei Huang's group at Yanshan University. Her major research interests focus on the synthesis and preparation of organic cathode materials for Li batteries.



Xinlei Xu obtained her B.S. degree in applied chemistry from Hebei University of Engineering in 2023. Now, she is a Master's candidate in Prof. Weiwei Huang's group at Yanshan University. Her main research focuses on the synthesis and fabrication of organic cathode materials for Li batteries.



Weizhe Gao is an undergraduate of Yanshan University, majoring in applied chemistry. Now, she is conducting battery-related research in Prof. Weiwei Huang's group.

2. Hydrogen Bonds Science in Organic Electrode Materials

Organic electrode materials (OEMs) stably store significant amounts of electrical energy through reversible redox reactions, achieving safe and stable energy supplies. Bond changes are involved in these redox reactions, making bond chemistry crucial in the reversible energy storage process of OEMs. The chemistry of covalent bonds, ionic bonds, and hydrogen bonds relate to the structural stability and reactivity of electrode materials, thus affecting the batteries' electrochemical performance.

Since the concept of hydrogen bonds was proposed, it has been widely applied in chemical science,^[23] materials science,^[24] biological science,^[25] and other fields. However, its roles in battery systems have only recently gained attention from



Qichun Zhang received his B.S. at Nanjing University in China in 1992, MS in physical organic chemistry at Institute of Chemistry, Chinese Academy of Sciences in 1998, MS in organic chemistry at University of California, Los Angeles (USA, 2003), and completed his Ph.D. in chemistry at University of California Riverside in 2007. He worked as a Postdoctoral Fellow (Oct. 2007–Dec. 2008) at Northwestern University. Since Jan. 2009, he joined School of Materials Science and Engineering at Nanyang Technological University (NTU, Singapore) as an Assistant Professor. On Mar 1st, 2014, he has promoted to Associate Professor with tenure. On Sep 1st, 2020, he moved to Department of Materials Science and Engineering at City University of Hong Kong as a full professor. From 2018 to 2021, he has been recognized as one of highly-cited researchers (top 1%) in cross-field in Clarivate Analytics. Currently, his research focuses on carbon-rich conjugated materials and their applications. Till now, he has published >550 papers and times cited >40000 (H-index: 114).



Weiwei Huang is a Professor at Yanshan University. She obtained her Ph.D. degree of physical chemistry at Nankai University in 2011. Then, she joined Prof. Jun Chen's group at Nankai University as a postdoctoral fellow. Since 2013, she joined the School of Environmental and Chemical Engineering at Yanshan University. She was a visiting scholar at Nanyang Technological University in 2019. Her research is focused on the organic electrode materials for Li/Na/K batteries.

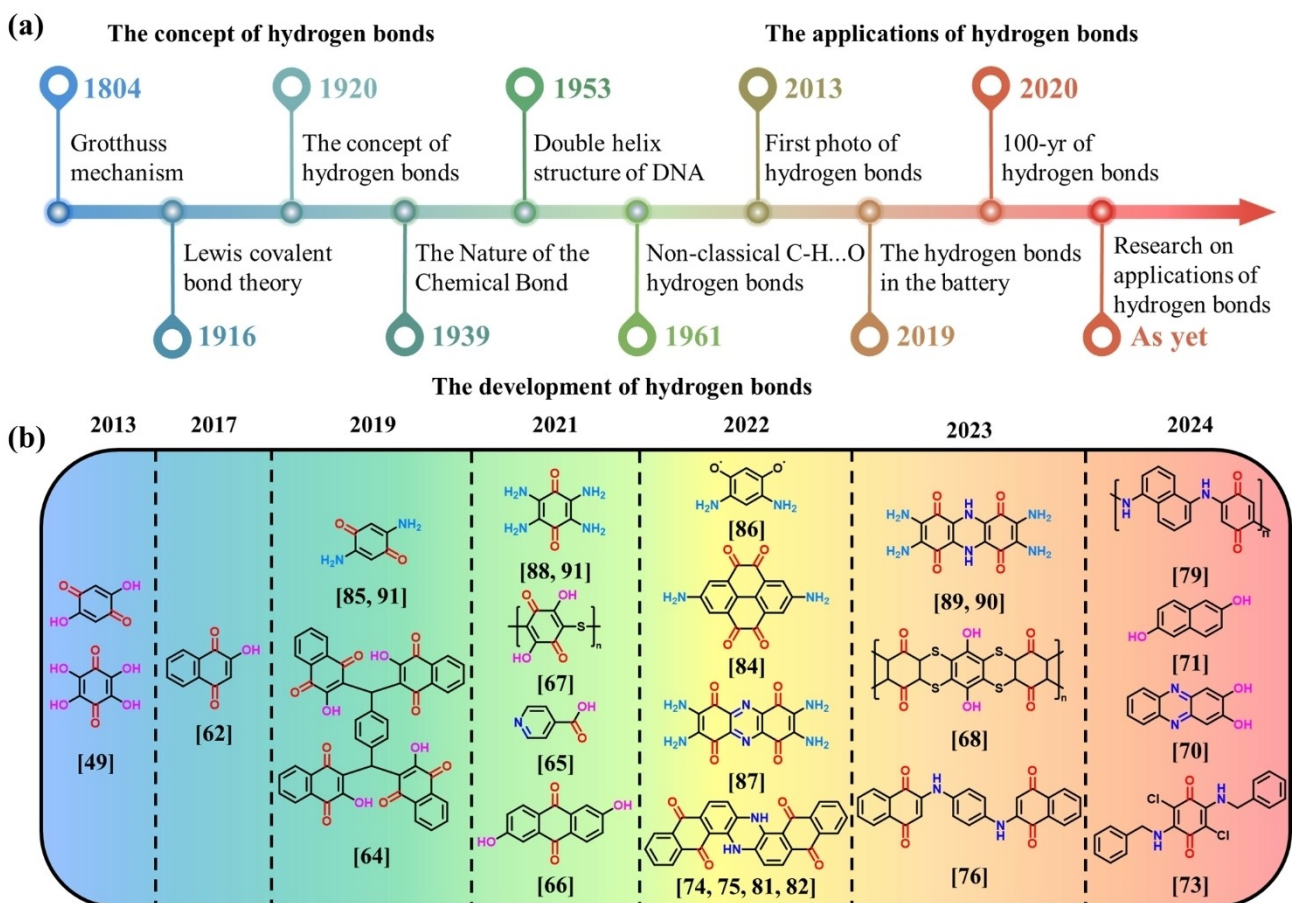


Figure 1. a) History of hydrogen bonds research and development. b) Some organic electrode materials are used for hydrogen bond research in batteries

researchers. Recent studies have demonstrated that hydrogen bond science significantly influences electrodes (e.g., adjusting charge distribution, stabilizing crystal structure, inhibiting materials dissolution, preventing materials pulverization, and speeding up diffusion kinetics) and electrolytes (e.g., optimizing plating/stripping processes, inhibiting side reactions and metal anodic corrosion, adjusting charge carrier transfer mechanisms and solvation structures).^[26] The study of hydrogen bond science in batteries will provide significant guidance for optimizing battery systems.

Hydrogen bonds typically form when substances are in liquid states,^[27] but they can also exist in crystalline or gaseous states. Thermal stability is one of the crucial criteria for evaluating the cyclic stability of OEMs across wide ranges of temperatures. The presence of Intra-HBs weakens intermolecular forces, generally lowering the melting and boiling points of these materials. Substances with Inter-HBs must overcome common intermolecular forces during melting or vaporization, and additional energy is required to break the hydrogen bonds, which slightly increases their melting and boiling points.^[28] Solubility is another important factor affecting the cyclic stability of OEMs. The creation of hydrogen bonds between the molecules of the solute and the solvent will increase the solubility of materials. However, strong hydrogen bonds within

or between materials can lead to bond saturation, inhibiting dissolution in electrolytes to some extent.^[29]

Up to now, the active sites of reported OEMs mainly include $\text{C}=\text{O}$,^[30] $\text{C}=\text{N}$,^[31] $\text{N}=\text{N}$,^[32] and $-\text{NO}_2$,^[33] among others. These active groups are primarily composed of elements with high electronegativity (e.g., N, O) and are excellent HBAs. Therefore, if material molecules contain HBDs, such as amino ($-\text{NH}_2$), imino ($-\text{NH}-$), or hydroxyl ($-\text{OH}$) groups, Intra-HBs or Inter-HBs can form through weak interactions, leading to special effects such as enhancing material stability,^[34] increasing the activity of active groups,^[35] and improving carrier diffusion.^[36] Although C–H in aromatic rings can sometimes act as unconventional weak HBDs, their role in battery systems is less significant than that of classical hydrogen bonds due to their weaker interaction forces. Consequently, few researchers have studied C–H as true HBDs.^[37] Notably, studies have shown significant distance-dependent thresholds in intramolecular interaction energies. Hydrogen bond energy is less than -1 kJ mol^{-1} when the interacting groups are separated by six or more rotating bonds but ranges between -5 and -9 kJ mol^{-1} for five or fewer rotors.^[38] Thus, hydrogen bonds are generally preferentially formed within molecules, with only very strong external HBAs able to compete with stronger internal hydrogen bonds. Intra-HBs can form four-membered,^[39] five-membered,^[40] six-membered,^[41] seven-membered,^[42] and other hydrogen bond

nets, with six-membered ring Intra-HBs being the most stable, as various studies have demonstrated.^[43]

Taking common carbonyl compounds as examples, these compounds offer significant advantages such as high theoretical specific capacity, designable structures, low price, and environmental sustainability. They constitute a substantial proportion of OEMs.^[44] The reversible conversion of carbonyl groups between their oxidized state ($\text{R}(\text{C}=\text{O})\text{R}'$) and reduced state ($\text{R}(\text{C}-\text{O}-\text{M}_x)\text{R}'$) facilitates the storage and release of electric charges, here, R and R' denote organic frameworks, and M represents ions such as H^+ , Li^+ , or Zn^{2+} , highlighting their effectiveness as active groups in OEMs.^[45] 1,4-benzoquinone (BQ) is a simple redox-active monomer in OEMs, notable for having a high voltage (2.7 V vs. Li^+/Li) and theoretical specific capacity (496 mAh g^{-1}). However, BQ sublimates easily in air, with noticeable sublimation occurring above 60 °C.^[46] Additionally, BQ or its discharge products dissolve significantly in the electrolyte, resulting in substantial capacity attenuation and poor electrochemical performance. Molecular structure design is considered an effective strategy to mitigate these issues,^[47] and introducing hydrogen bond donors has gained increasing interest in recent years due to its special benefits in different molecular structure design techniques.^[48]

2.1. Introduction of BQ-Based Materials with -OH Groups

Hydroxyl is a strong HBD, and up to four -OH groups can be introduced on the benzoquinone unit, and the introduction of -OH groups can greatly improve the instability of the benzoquinone intrinsic properties. Hanyu^[49] studied the performance of 2,3-dichloro-5,6-dicyano-1,4-benzoquinone (DDQ), 2,5-dihydroxy-1,4-benzoquinone (DHBQ), and 2,3,5,6-tetrahydroxy-1,4-benzoquinone (THBQ) in quasi-solid state lithium-ion batteries in 2012, and found that the energy density of DHBQ is 20–30% higher than THBQ in the solid electrolyte system, which is less problematic compared to dissolution and capacity decay in the organic electrolyte system. Unfortunately, their focus on the solid electrolyte to prevent material dissolution did not include long-term cycle tests or additional characterization tests, thus limiting the information obtained about the electrode materials. However, increasing studies have been conducted on the electrochemical performance of DHBQ, THBQ, and their derivatives in recent years. DHBQ, which introduces two para-hydroxyl groups based on the BQ unit, has a lower theoretically specific capacity of 382 mAh g^{-1} , which is related to the -OH groups' addition. The $\text{C}=\text{O}$ and -OH bonds can form coordination compounds with various metal ions, making DHBQ a standout among common organic ligands due to its low molecular weight and broad applicability. It is particularly suitable for constructing high-capacity MOF-type cathode materials. Kon et al.^[50] studied the performance of a one-dimensional structural complex formed by DHBQ with Fe^{2+} in lithium batteries in 2021. $\text{Fe}(\text{DHBQ})(\text{H}_2\text{O})_2$ is formed via the coordination of one Fe^{2+} core with two neighboring DHBQ²⁻ ligands and two crystal waters. After the process of drying, the material achieved the reversible capacity of 181 mAh g^{-1} , with

an average discharge voltage of around 2.1 V vs. Li^+/Li . The following year, Cai et al.^[51] synthesized and studied the performance of a three-dimensional (3D) structural complex formed with Fe^{3+} in lithium-ion batteries (LIBs). The coordination between one Fe^{3+} center and three DHBQ^{2/3-} ligands increased the average discharge voltage to 2.43 V and resulted in the high reversible capacity of 285 mAh g^{-1} . Additionally, the properties of complexes formed by DHBQ with $\text{Ni}^{[52]}$, $\text{Cu}^{[53]}$ and other ions in batteries have been studied, yielding significant results. In 2024, Zheng^[54] based on Honma's research, investigated the electrochemical performance of DHBQ in all-solid-state lithium batteries (ASSLBs). They put forward an electrode/electrolyte interface scheme and established the π -d conjugate coordination structure between the cathode electrodes and the electrolytes, demonstrating good redox reversibility. The strong combination of DHBQ with PVDF- $\text{Li}_{3x}\text{La}_{2/3-x}\text{TiO}_3$ (LLTO) can withstand the volume change of DHBQ during electrochemical cycles while maintaining low interfacial resistance, thereby ensuring good cyclic stability and rate performance in ASSLBs.

THBQ introduces four -OH groups into the BQ unit, resulting in the theoretical specific capacity of 311 mAh g^{-1} . The introduction of four hydroxyls enhances its potential as an organic ligand for metal ions. THBQ has been reported to be used in batteries with metal coordination structures, including those with $\text{Al}^{[55]}$ and $\text{Cu}^{[56]}$ ions, demonstrating excellent performance. These findings underscore the significant potential of THBQ in the battery field.

2.2. Introduction of BQ-Based Materials with -NH₂ Groups

In addition to hydroxyl groups, amino groups also serve as strong HBDs. 2,5-Diamino-1,4-benzoquinone (DABQ), with two para-amino groups introduced into the BQ unit, has a theoretical specific capacity of 388 mAh g^{-1} . Compared with 2,3,5,6-diamino-1,4-benzoquinone (TABQ), which introduces four -NH₂ groups, DABQ is less suitable as an organic ligand for metal ions due to the presence of only two -NH₂ groups. However, DABQ's performances in batteries have been thoroughly studied, and the effectiveness of its Intra-HBs and Inter-HBs in battery cycles has been verified. Although the theoretical specific capacity of TABQ decreases to 319 mAh g^{-1} after the introduction of four -NH₂ groups into the BQ unit, TABQ has demonstrated excellent performance in batteries and serves as an effective organic ligand due to the presence of two pairs of para-amino groups. Geng^[57] designed a new two-dimensional (2D) iron(III)-tetraamino-benzoquinone (Fe-TABQ) with dual redox centers of Fe^{3+} and TABQ ligands for high-capacity and stable Li^+ storage. The Fe-TABQ chains are connected by multiple hydrogen bonds, forming the extended π -d conjugated 2D structure with a high capacity of 251.1 mAh g^{-1} and an energy density of 577.5 Wh kg^{-1} . Its capacity retention rate exceeds 95% after 200 cycles at different current densities. Furthermore, polymers synthesized by coordinating TABQ with metal ions such as $\text{Ni}^{[58]}$, $\text{Co}^{[59]}$, and $\text{Cu}^{[60]}$ ions have also been studied, demonstrating TABQ's significant development potential in the battery field.

From the above, it is evident that while the introduction of $-\text{OH}$ or $-\text{NH}_2$ groups reduces theoretical capacity, it enhances the materials' functionality and battery performance. The introduction of HBDs significantly expands the research scope of OEMs. The hydrogen bond mechanisms in DHBQ, THBQ, DABQ, and TABQ have been extensively studied, and the following sections will detail hydrogen bonds in OEMs from the perspective of different HBDs (Figure 2).

3. Hydroxy ($-\text{OH}$) Hydrogen Bonds in Organic Electrode Materials

The hydroxyl group is made up of the covalent bonds formed between the oxygen and hydrogen atoms, which can donate a hydrogen atom to more electronegative atoms through weak interaction forces. In battery systems, the hydroxyl groups can form hydrogen bond networks with active groups, electrolytes, or binders, thereby strengthening the stability of the electrodes. The self-healing mechanism of the hydrogen bond networks is crucial for preventing material pulverization and shedding due to volume changes, and it also facilitates rapid ion transport.^[61] However, it may occupy active sites, leading to reductions in actual capacity. Additionally, as an electron-donating group, an increased number of hydroxyl groups can lower the reduction potential of the materials. Nevertheless, the electron-donating nature also enhances the activity of the electrode material's active sites, thus improving the battery's rate performance and reversible cycle efficiency.

3.1. The Role of $-\text{OH}$ Hydrogen Bonds in Proton-Free Electrolytes

In proton-free electrolytes, the hydroxyl group can not serve as the active center for reversible electrochemical energy storage, and thus it is generally not considered an active site, which results in declines in the theoretical capacity of the materials. However, the hydrogen bond networks composed of the materials with H provided by the $-\text{OH}$ can increase the thermodynamic stability of the material, which manifests as long-term cyclic stability and rate stability of materials. Lee and Park^[62] studied the performance of LIBs of 1,4-naphthoquinone (NQ), 2-methyl-1,4-naphthoquinone (menadione), and 2-

hydroxy-1,4-naphthoquinone (Lawson). Lawson achieved the best performance thanks to the construction of the hydrogen bond networks (Figure 3a). The introduction of $-\text{OH}$ groups significantly decreased the reduction potential (from 2.53/2.32 V of NQ to 2.37/2.03 V of Lawson). Compared to menadione and unmodified NQ, Lawson has ionic and electrical conductivities that are three to five times higher, all attributed to the introduction of $-\text{OH}$, and the hydrogen bond networks provided by $-\text{OH}$ facilitate rapid ion migration. Notably, during the first five cycles, Lawson takes place the irreversible structural transition from $-\text{OH}$ to $-\text{OLi}$, resulting in high discharge capacity and low coulomb efficiency (CE) in the initial cycle. This explains the phenomenon wherein some hydroxy-containing materials have high initial capacity in some systems of batteries but maintain reversible cycles at a lower capacity. Additionally, research was done on how $-\text{OH}$ affected the functionality of potassium-ion batteries (PIBs). Slesarenko et al.^[63] designed and synthesized octahydroxytetraazapentaene (OHTAP) for application in LIBs and PIBs. Theoretically, OHTAP can reach the capacity of 665 mAh g^{-1} by transferring 10 electrons. In practice, OHTAP achieved capacity performance close to the theoretical capacity at low current density rates, but in subsequent cycles, the capacity gradually decreased until it stabilized. Similar results were observed for PIBs. For LIBs alone, the final capacity stabilizes at 200 mAh g^{-1} . The authors attributed this phenomenon to material dissolution. However, studies have shown that OHTAP is insoluble in commonly used organic electrolytes, with only its octolithium salt (LiOTAP) dissolving slightly, suggesting that the experimental phenomenon can not be explained by dissolution alone. This capacity corresponds to the four-electron transfer, and the experimental results can be explained by Lee and Park's theory that irreversible $-\text{OH}$ to $-\text{OLi}$ transformation occurred in the first dozens of cycles, and the real active sites are the $\text{C}=\text{N}$ groups.

In addition to the significant role of the hydrogen bond network in LIBs and PIBs, its application in sodium-ion batteries (SIBs) has also been systematically studied. Miroshnikov et al.^[64] synthesized tetrakislawson (TKL) in the water/ethanol solution using the one-step method and examined its performance in SIBs. At 50 mA g^{-1} , the built SIBs reached the maximum capacity of 237 mAh g^{-1} , indicating that the existence of hydrogen bonds inhibited the dissolution of the electrode materials in the electrolytes (Figure 3b). Density functional theory (DFT) calculations revealed that Na^+ was connected at the interface of the hydroxyl/carbonyl sites of the two lawson substructures. With the coordination of two Na^+ , the bond energy of the $\text{O}-\text{H}\dots\text{O}$ site was significantly enhanced, indicating that the strengthening of hydrogen bonds and the increase in Na^+ coordination number would lead to the distortion of the TKL molecular structure. This distortion ultimately prevented the entry of the third Na^+ into the coordination, resulting in the relative instability of 3NaTKL . This conclusion was further corroborated by the equilibrium between 3NaTKL and 2NaTKL observed in NMR results. The reversible transfer of two Na^+ with two electrons was further shown by kinetic investigations employing the galvanostatic intermittent titration technique (GITT) and cyclic voltammetry (CV). These findings reveal that while



Figure 2. The $-\text{OH}$, $-\text{NH}_2$ derivatives of BQ, and possible structures of unimolecular hydrogen bonds.

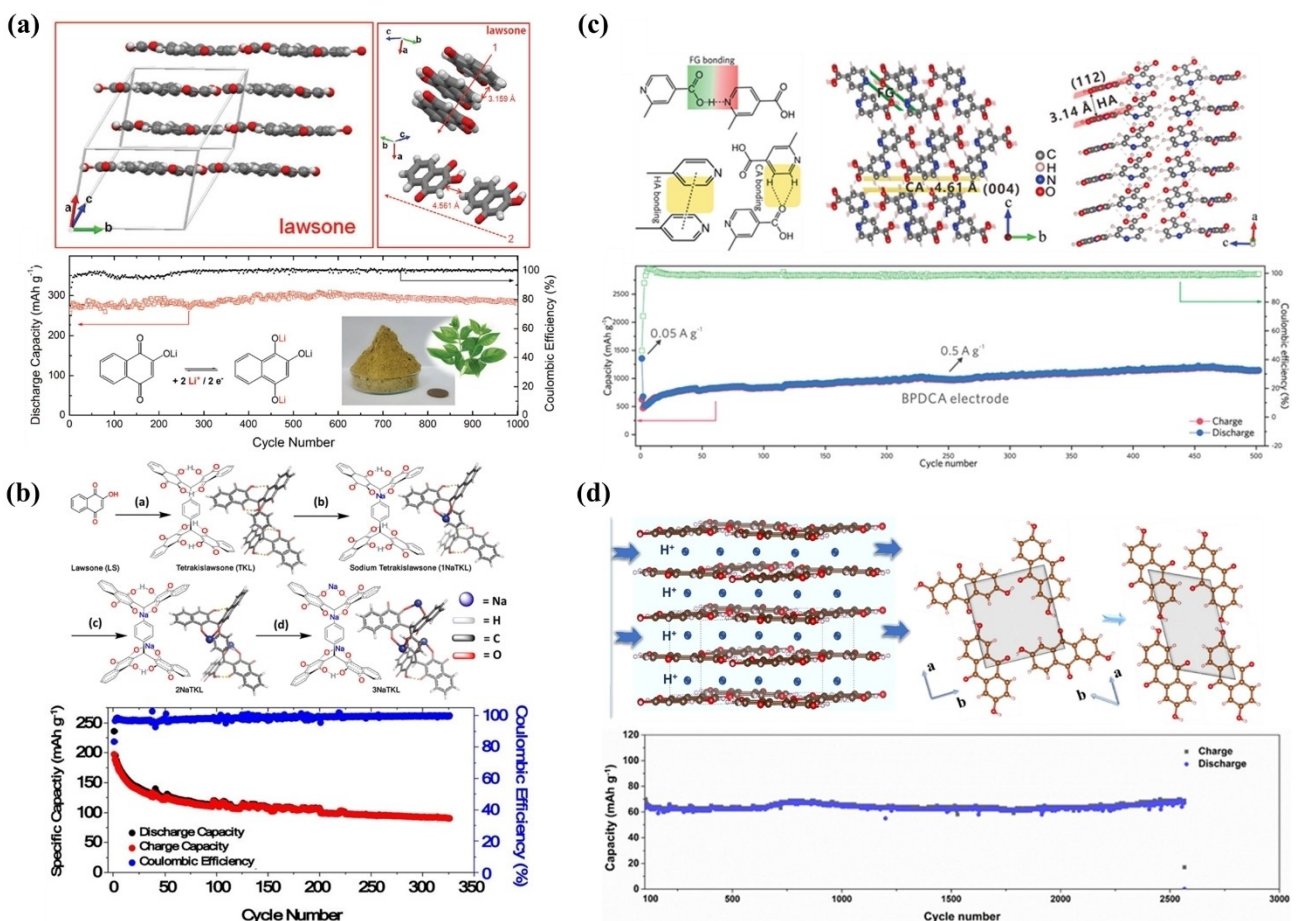


Figure 3. a) The stack structure of Lawsone and cyclic performance of Li | Lawsone batteries at 0.5 C. Reproduced from Ref.^[62] with permission, Copyright (2017) Wiley-VCH. b) The sodium insertion mechanism of TKL hydrogen bonds break and cyclic performance of Na | TKL batteries at 50 mA g⁻¹. Reproduced from Ref.^[64] with permission, Copyright (2019) American Chemical Society. c) The hydrogen bonds stacking channel of BPDCA and cyclic performance of Li | BPDCA batteries at 0.5 A g⁻¹. Reproduced from Ref.^[65] with permission, Copyright (2021) Wiley-VCH. d) The packing structure of DHAQ and cyclic performance of DHBQ | Mn²⁺ batteries at 1.13 A g⁻¹. Reproduced from Ref.^[66] with permission. Copyright (2021) Elsevier B.V.

hydrogen bonds prevent the electrode materials from dissolving, they may also lower the number of available active sites, leading to lower capacity performance and energy power density.

The ion transport channel formed by the hydrogen bond networks significantly enhances ion transport rates. It is well known that carrier ions are embedded along one-dimensional channels formed by functional groups (FG), however, FG channels limit the high-speed conduction of ions. Molecular stacking offers a strategy to overcome these limitations. Conjugated alkene hydrogen bonds (CA) and heterocyclic aromatic stack bonds (HA) create additional channels, facilitating rapid insertion and removal of carrier ions. Through FG, CA, and HA 3D migration channels, certain organic compounds can be activated as excellent electrochemical energy storage materials, promoting rapid ion transfer and high utilization of active sites. Hu et al.^[65] investigated the performance of LIBs using the heterocyclic organic molecule

2,2'-bipyridine-4,4'-dicarboxylic acid (BPDCA). Thermogravimetric analysis (TGA) showed that BPDCA was thermally stable below 350 °C, and electrolyte dissolution experiments con-

firmed its chemical inertness in the electrolytes. The co-activation of functional groups and weak bond structures, the specific capacity and rate capability of the organic electrode significantly improved by specifically the R₁-C=C(X)...X-R₂ hydrogen bonds and C₅H₃N...NH₃C₅ interlayer bonds. Consequently, the excellent rate performance (478.9 mAh g⁻¹ at 20 A g⁻¹) and extremely high reversible capacity (1206 mAh g⁻¹ at 0.5 A g⁻¹) were achieved by the BPDCA electrode (Figure 3c).

3.2. The Role of -OH Hydrogen Bonds in Proton-Containing Electrolytes

The application of -OH hydrogen bond donors (HBDs) has been studied in both proton-free and proton-containing electrolytes. In proton-containing electrolytes, the hydrogen bond networks formed between the HBDs and HBAs may facilitate the Grotthuss mechanism of proton transfer, enhance the ion shuttle rate, and promote charge transfer. Additionally, the carbonyl and hydroxyl groups can undergo reversible conversion, resulting in increased cycling capacity. Yu et al.^[66] explored

the potential of 2,6-dihydroxy-anthraquinone (DHAQ) for proton energy storage. By van der Waals forces and hydrogen bond networks, DHAQ creates the layered crystal structures and maintains interlayer integrity during cycling. Their results show that the aromatic rings, rather than the C=O group, are the redox core of DHAQ, which may be associated with the Grotthuss mechanism facilitated by the hydrogen bond networks. The half-organic proton battery was built with the cathode of Mn²⁺ solution and the anode of DHAQ, and achieved the discharge platform voltage of approximately 1.02 V, after 2600 cycles with capacity retention rates of 100% (Figure 3d).

The reversible conversion of C=O and -OH groups endows the material with strong self-regulation capabilities, maintaining good performance under various cycling conditions. Sun et al.^[67] synthesized poly(2,5-dihydroxy-1,4-benzoquinone sulfide) (PDBS) through molecular polymerization and applied it to the study of aqueous zinc-ion batteries (AZIBs). The ductile of the PDBS polymer chain can adapt to the distortion of the polymer structure when the materials are insertion or deinsertion the ion, facilitating the insertion and deinsertion of Zn²⁺. The reversible transformation of C=O and -OH groups in OEMs in aqueous electrolytes grants PDBS unique advantages in binding polyvalent metal ions. The presence of sulfur bonds and -OH groups maintain the material's structure and increase the reactivity of carbonyl groups, allowing PDBS to sustain 2000

cycles at 2 A g⁻¹ and preserve a high reversible capacity of 260 mAh g⁻¹. Similarly, Sun et al.^[68] designed polytetrafluorohydroquinone (PTFHQ), a sulfur-bonded Z-folded hydroxyl polymer, and studied the electrochemical properties of AZIBs as cathode electrodes. They found that during the cycle, the -OH groups in PTFHQ can be partially in situ oxidized to active C=O groups, thus possessing the ability to bind to Zn²⁺. Concurrently, the remaining -OH groups act as proton carriers, ensuring PTFHQ's activity in weakly acidic electrolytes and improving its stability. As a hydrophilic group, -OH also enhances the material's hydrophilicity, thereby accelerating Zn²⁺ transport. As a result, PTFHQ attained remarkable cycle stability (92% capacity retention after 3400 cycles), excellent rate performance (91% capacity retention at 20 A g⁻¹), and high reversible capacity (215 mAh g⁻¹ at 0.1 A g⁻¹).

3.3. The Influence of the Number of -OH Hydrogen Bonds on the Properties Of Electrode Materials

To optimize the properties of the material, it is essential to introduce an appropriate number of -OH groups. Introducing too many hydroxyl groups will increase the material's dissolution, leading to unstable cycles and low capacity performance due to the simultaneous occupation of excessive redox-active groups. Conversely, introducing too few -OH groups may prevent the materials from fully utilizing their potential and functioning optimally. Therefore, only by incorporating a reasonable number of hydroxyl groups can the material's properties be optimized. Lap et al.^[69] synthesized a series of bio-based polyhydroxyanthraquinone (PHAQ) materials, including

2,3,6,7-tetrahydroxyanthraquinone (THAQ), 1,2,3,5,6,7-hexahydroxyanthraquinone (HHAQ), and 1,2,3,4,5,6,7,8-octahydroxyanthraquinone (OHAQ), as well as their polymers. They studied the performance of these materials as high-voltage OEMs for batteries. The findings revealed that the anthraquinone core's electron-absorbing action was counteracted by the electron-donating -OH groups, thereby reducing the reduction potential with the increased number of -OH groups. The optimal number of -OH groups enhances the batteries' discharge voltage, but an excessive number causes significant material dissolution in the organic electrolytes. In addition to C=O groups, imine groups (C=N) are also common active functional groups in OEMs. Lap's conclusions were also verified in materials where C=N groups were active. Cui et al.^[70] synthesized three phenazine derivatives with varying -OH group quantities — 1,2-dihydroxyphenazine (PZ-2OH), 2-hydroxyphenazine (PZ-OH), and phenazine (PZ) for use as anode electrode materials in alkaline aqueous batteries (ANABs). Introducing -OH groups to phenazine, which serve as donor groups for electrons, significantly reduced the discharge potential (vs. Hg/HgO) from -0.78 V (PZ) to -0.9 V (PZ-OH) and -1.07 V (PZ-2OH). Additionally, phenazine derivatives with -OH groups exhibited superior rate properties and lower charge transfer resistance compared to phenazine, and the intermolecular interaction through the -OH functional group supplied quick charge transfer pathways. Ultimately, PZ-2OH demonstrated robust cyclability (more than 9000 cycles), high power density (26.2 kW kg⁻¹ at 10 A g⁻¹), and high reversible capacity (178 mAh g⁻¹ at 0.2 A g⁻¹) (Figure 4a).

3.4. The Influence of the Location of -OH Hydrogen Bonds on the Properties of Electrode Materials

Apart from the quantity of hydroxyl groups impacting the material's functionality, the location of these groups also influences battery performance. Zhao et al.^[71] investigated the electrochemical characteristics of six different kinds of dihydroxynaphthalenes (DHNs) and discovered that DHNs undergo in-situ electropolymerization during charge and discharge cycles, leading to capacity attenuation. However, 2,6-DHN exhibits a higher polymerization energy barrier, resulting in superior cathode performance in proton batteries. It accomplished the outstanding charge-discharge capacity (91.6 mAh g⁻¹ at 1 A g⁻¹) and the high redox potential of 0.84 V vs. SHE. To enhance its electrochemical performance, 2,6-DHN is compounded with reduced graphene oxide (rGO), and even after 12000 cycles at 5 A g⁻¹, the 2,6-DHN/rGO electrode maintained the specific capacity of 89 mAh g⁻¹. The presence of polyhydroxy groups in DHNs constructs hydrogen bond networks, which, along with van der Waals forces, contribute to the formation of rapid proton transfer channels with good long-range order. This enables all-organic proton batteries paired with 2,6-dihydroxyanthraquinone (DHAQ) anode to achieve faster proton transfer, high battery voltage (0.85 V), impressive energy/power density (0.8 Wh kg⁻¹/850 W kg⁻¹), long-term cycle stability (70.9% capacity retention after 1000 cycles), and high initial specific capacity (83.3 mAh g⁻¹ at 1 A g⁻¹) (Figure 4b).

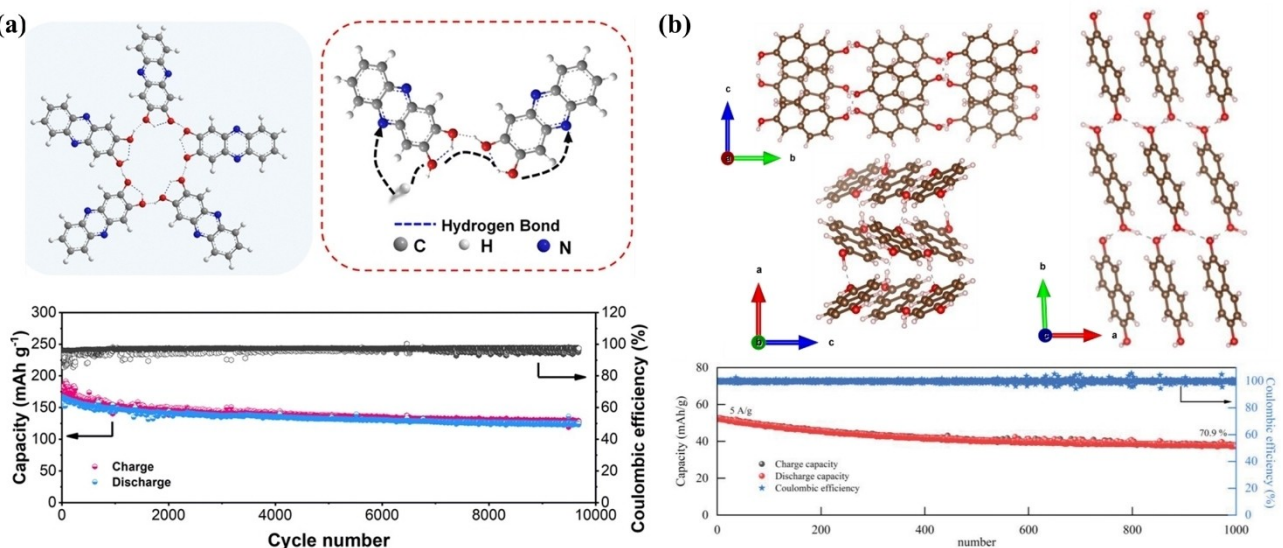


Figure 4. a) The hydrogen bonds structure of PZ-2OH and cyclic performance of PZ-2OH || Ni(OH)₂ batteries at 1 A g⁻¹. Reproduced from Ref.^[70] with permission. Copyright (2024) The Royal Society of Chemistry. b) The stack structure of 2,6-DHN and cyclic performance of 2,6-DHN/rGO || 2,6-DHAQ batteries at 5 A g⁻¹. Reproduced from Ref.^[71] with permission, Copyright (2024) Wiley-VCH.

4. Imino (–NH–) Hydrogen Bonds in Organic Electrode Materials

Similar to the –OH group, the –NH– group can provide a hydrogen atom for bonding with a more electronegative atom or group through weak interactions. However, due to the higher electronegativity of O compared to N, the hydrogen bond networks constructed in battery systems will exhibit different effects. It has been demonstrated that the –NH– groups can facilitate proton conduction, enabling the reversible conversion of –C–NH– with –C=N–,^[72] and this suggests the potential of –NH– for proton storage as the redox-active center in the electrochemical process. Current studies on –NH– bonded substances primarily focus on Intra-HBs. Nonetheless, when the –NH– groups are distant from electronegative atoms within the molecule, they can also form Inter-HBs. The role of –NH– hydrogen bonds will vary between proton-free and proton-containing electrolyte systems. Therefore, studying the role of –NH– hydrogen bonds in OEMs during the battery cycle is of great significance.

4.1. The Role of –NH– Hydrogen Bonds in Proton-Free Electrolytes

Hydrogen bonds are essential to stabilize the electrode material structure and inhibit the dissolution of the materials, due to the lack of protons in the proton-free electrolyte. However, the presence of hydrogen bonds may occupy active sites, resulting in low utilization of these sites. Hiltermann et al.^[73] utilized p-chloranil (PC), 2,3-dichloro-5,6-dicyano-p-benzoquinone (DDQ), and vanillin to design and synthesize five different quinone derivatives to look into how battery performance is affected by Intra-HBs. The dissolution of these five materials in the elec-

trolyte composed of ethylene carbonate (EC), diethyl carbonate (DEC), and 1.0 M LiPF₆ was examined. The results indicated that quinones 1, 2, and 3 exhibited low solubility in the electrolyte. However, quinone 4 showed significant dissolution in the polar electrolyte after ultrasound treatment, and quinone 5 exhibited the most severe dissolution due to the absence of hydrogen bond functions. The optimized structures of quinones 1 to 4, determined by the DFT method, showed the expected Intra-HBs between the C=O and the –NH–, forming planarized intramolecular 5-membered rings. ¹H NMR spectroscopy also confirmed the existence of Intra-HBs. The authors objectively analyzed the different dissolution behaviors of the materials without exaggerating the role of hydrogen bonds. They proposed that the planar aromatic rings in quinones 2 and 4 might cooperate with the conductive carbon framework of the cathodes, diminishing their dissolution in the electrolytes. In contrast, the non-polar aliphatic cyclohexyl groups in quinones 1 and 3 have restricted solvency in polar electrolytes, contributing to their low solubility. Additionally, the addition of halogen atoms and the large molecular mass of quinones 1 to 4 also contributed to their low solubility. However, the authors were not excluded from conducting more in-depth studies of these factors, indicating that the work has certain limitations and warrants further investigation.

When the batteries are charged and discharged in proton-free electrolytes, metal ions may replace hydrogen, forming new bonds that stabilize the materials. Shi et al.^[74] oxidized indanthrone (IDT) to oxidized indanthrone (oIDT) through the one-step oxidation process and investigated the application of both materials in LIBs. With a high reversible capacity of 273 mAh g⁻¹ and an average discharge voltage of 2.45 V at 50 mA g⁻¹, oIDT displayed good electrochemical performance in the optimum voltage range of 1.3–3.8 V vs. Li⁺/Li. Furthermore, during extended cyclings (76% after 1000 cycles at 500 mA g⁻¹)

and high currents (75% at 2000 mAh g⁻¹), it demonstrated impressive capacity retention. Conversion of dihydropyrazine to pyrazine improved structural stability while charging and discharging and increased theoretical capacity and redox potential in comparison to IDT. The innovative concept of using lithium bonds instead of hydrogen bonds to stabilize the structure in organic electrolytes provided theoretical support for the observed structural stability of certain small molecules in such environments. In the same year, Zhang et al.^[75] achieved the oxidation of IDT to oIDT during the process of charging and discharging by adding LiNO₃ to the electrolytes. The fact that IDT has hydrogen bonds indicates its potential as a structurally stable electrode material (Figure 5a). However, the occupation of redox-active sites by hydrogen bonds limits the actual capacity performance of IDT. The in-situ oxidation of NO₃⁻ during cycling converts IDT to the oIDT structure, significantly improving capacity performance. The concurrence of similar findings in the same journal within almost the same year by two different studies is an interesting coincidence.

The small molecule 2,2-(1,4-phenylbis (azo)) dinaphthalene (DNQPA), characterized by Intra-HBs, has been employed in the performance study of LIBs.^[76] The reason behind DNQPA's low solubility in the electrolyte and structural stability during the cycling process is the establishment of Intra-HBs. The strong hydrogen bonds between DNQPA and reduced graphene oxide (rGO) via —NH— groups, along with enhanced π-π interactions, significantly mitigate the dissolution of DNQPA in the DOL/DME electrolytes. As a result, the DNQPA/rGO composite showed excellent cyclic stability, maintaining 215.8 mAh g⁻¹ after 9000 cycles at 5 A g⁻¹ with an 85.6% capacity retention rate. It also had a high initial capacity (290 mAh g⁻¹ at 1 A g⁻¹) and respectable rate performance (252 mAh g⁻¹ at 5 A g⁻¹) (Figure 5b).

The reduced availability of active sites as a result of molecular aggregation is one of the primary causes of polymers' restricted usage. The Intra-HBs are effective at preventing polymer aggregation, according to recent research. Tao's

team^[77] designed and synthesized strong intermolecular interactions polymer (poly-(tetraminobenzoquinone-alt-2,5-dihydroxy-1,4-benzoquinone, PBQ). Almost all of the active sites of PBQ are exposed, resulting in extremely high active sites utilization (99.8%, 252.2 mAh g⁻¹ at 0.1 A g⁻¹) and the fast ionic diffusion (1.9×10⁻⁸ cm² s⁻¹), and stable cycles (98.6% at 1 A g⁻¹ after 400 cycles).

4.2. The Role of —NH— Hydrogen Bonds in Proton-Containing Electrolytes

When protons are present in the electrolyte, the —NH— group can store proton energy or combine with anions as the active sites of the p-type reaction to achieve reversible energy storage. More commonly, —NH— groups form hydrogen bond networks that facilitate proton energy storage. Geng et al.^[78] studied the electrochemical properties of 1,1'-iminodianthraquinone (IDAQ)/rGO composites as cathode electrodes for AZIBs. They discovered that IDAQ/rGO has remarkable stability, maintaining 96% capacity after 5000 cycles. XPS and FTIR analyses were used to investigate the ion storage process in IDAQ materials, confirming that carbonyl groups serve as the active sites of the reaction. Due to the smaller volume of H⁺ compared to Zn²⁺, H⁺ can also react with carbonyl groups. Cyclic voltammetry (CV) curves showed overlapping main peaks in dilute CF₃SO₃H and Zn(CF₃SO₃)₂ electrolytes, and a constant current charge-discharge (GCD) curve platform was observed in 3 M CF₃SO₃H, collectively proving the co-intercalation mechanism of H⁺ and Zn²⁺. The synergistic mechanism of Zn²⁺ and H⁺ in IDAQ/rGO was further explored through theoretical calculations, which indicated that the most likely product following discharge was IDAQ₂(H⁺)₆(Zn²⁺).

The Intra-HBs formed by —NH— groups significantly enhance charge transfer and improve the dynamics of energy storage in materials. Sun et al.^[79] designed and synthesized a quinone polymer H-PNADBQ using a strategy that incorporates Intra-

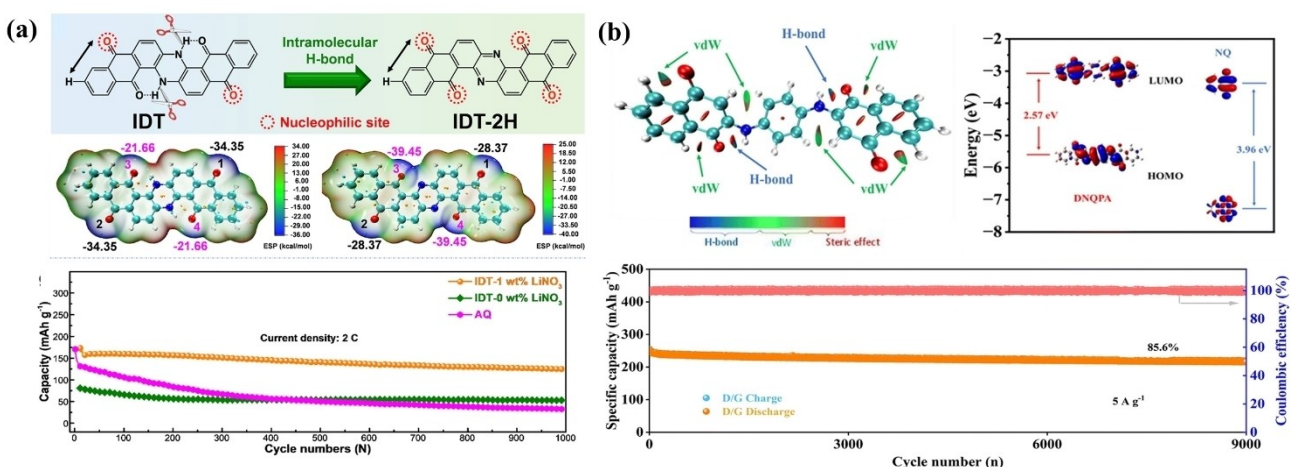


Figure 5. a) The hydrogen bonds structure of IDT and cyclic performance of Li | IDT batteries at 2 C. Reproduced from Ref.^[75] with permission. Copyright (2022) Elsevier B.V. b) The hydrogen bonds structure of DNQPA and cyclic performance of Li | DNQPA batteries at 5 A g⁻¹. Reproduced from Ref.^[76] with permission. Copyright (2023) The Royal Society of Chemistry.

HBs. The hydrogen bonds formed between C=O and –NH– groups were calculated using the atoms-in-molecules (AIM) theory and confirmed by FTIR analysis. H-PNADBQ's dipole moment was lowered by these Intra-HBs, resulting in its low solubility in aqueous solutions, and a high decomposition temperature (254°C) as shown by TGA. Furthermore, the H⁺/Zn²⁺ co-insertion mechanism of H-PNADBQ was elucidated using ex-situ FTIR, XRD, XPS, TEM-EDS, and SEM. Intra-HBs stabilized the molecular structure, reduced dissolution by lowering the electrostatic potential (ESP) of reactive sites and molecular polarization, enhanced electronic conductivity, and accelerated charge transfer by increasing the π -conjugation structure. Consequently, at high loading conditions (5 and 10 mg cm⁻²) H-PNADBQ exhibits a high rate capacity (137.1 mAh g⁻¹ at 25 A g⁻¹) (Figure 6a).

Generally, organic small molecules in electrolytes show decreased electrochemical properties due to molecular dissolution.^[80] However, the presence of –NH– hydrogen bonds enables small molecules to exhibit stable cyclic properties. Geng et al.^[81] studied the electrochemical properties of 6,15-

dihydrodinaphtho[2,3-a'2',3'-h]phenazine-5,9,14,18-tetraone (DNPT) and rGO composite as the cathode electrode of AZIBs. With 1000 cycles at 500 mA g⁻¹ (20 C), DNPT/rGO demonstrates good rate performance and stability, reaching a capacity of 120 mAh g⁻¹. The cooperative processes between H⁺ and Zn²⁺ in DNPT/rGO were discussed in detail through ex-situ analysis and DFT calculations. C=O groups were found to be the active centers in ex-situ experiments, and the activation process was because the phenol type and quinone type underwent the reversible structural transition. DFT was used to examine three potential discharge processes of DNPT₂(H⁺)₄(Zn²⁺)₂, DNPT₂(H⁺)₆(Zn²⁺), and DNPT(H⁺)₄. In charge and discharge, the optimal structure of DNPT₂(H⁺)₄(Zn²⁺)₂ is indicated by the binding of two DNPT molecules with one Zn²⁺ and six H⁺. Recently, the use of IDT in electrochemical energy storage was investigated by Peng et al.,^[82] proposing and verifying the feasibility of its bipolar energy storage. The p-type energy storage of the dihydropyrazine part and the n-type energy storage of the anthraquinone part enabled the assembled symmetric battery to achieve the output voltage of 0.62 V and

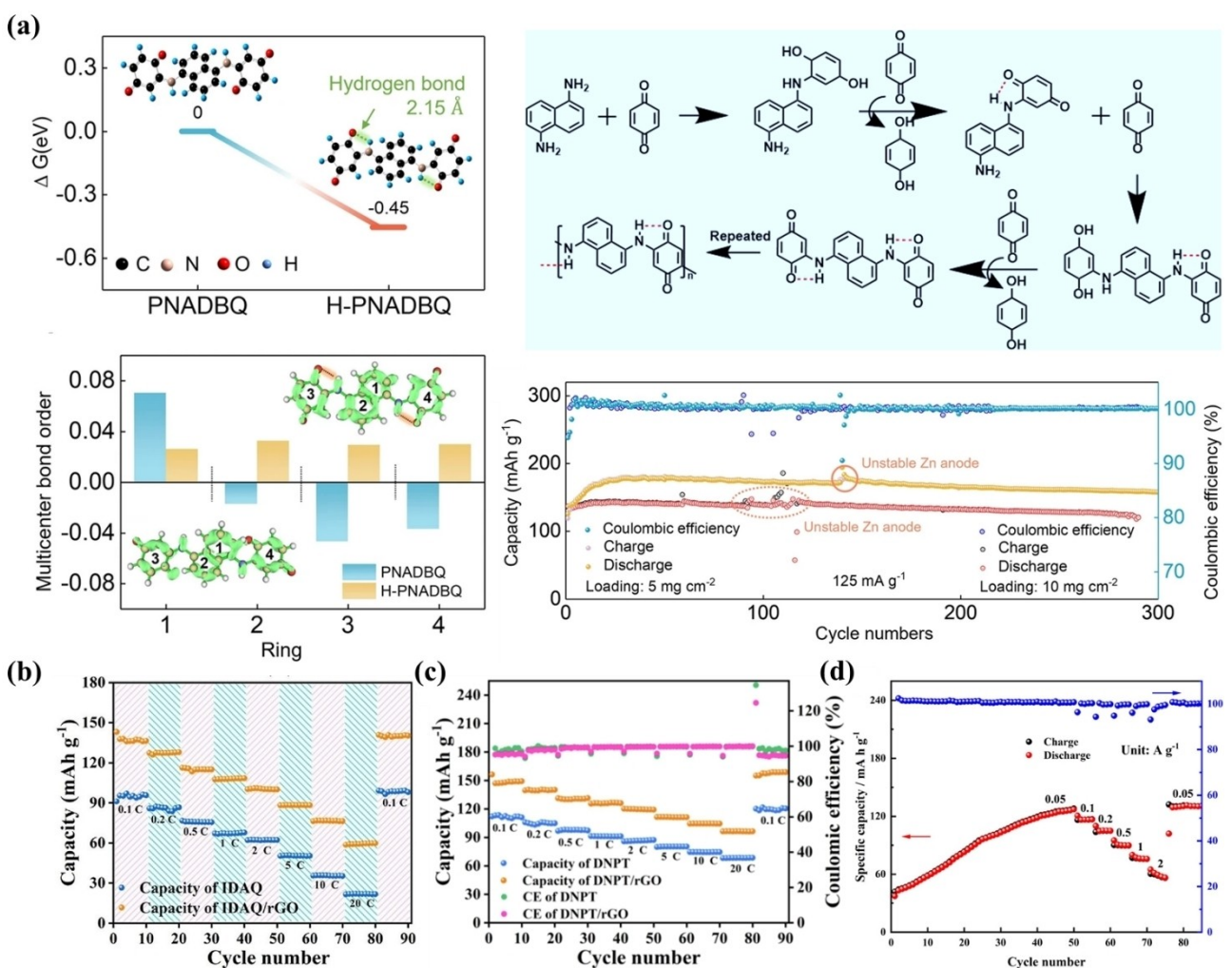


Figure 6. a) The hydrogen bonds structure of H-PNADBQ and cyclic performance of Zn||DNQPA. Reproduced from Ref.^[79] with permission. Copyright (2024) Springer Nature. b) The rate performance of Zn||IDAQ. Reproduced from Ref.^[78] with permission, Copyright (2022) American Chemical Society. c) The rate performance of Zn||IDT. Reproduced from Ref.^[81] with permission. Copyright (2022) Elsevier B.V. d) The rate performance of Zn||DADB. Reproduced from Ref.^[83] with permission, Copyright (2022) American Chemical Society.

provide the specific capacity (139 mAh g^{-1} at 0.1 A g^{-1}), with the capacity retention rate (79% after 600 cycles at 2 A g^{-1}).

The electrochemical properties of 8, 21-dihydronaphtho-[2,3-a]naphtho[2',3':7,8]quinoxalino[2,3-i]phenazine-5,11,16,22-tetraone (DADB), featuring a dihydropyrazine structure in AZIBs, were also investigated. 2,5-dihydroxy-1,4-benzoquinone (DHBQ), and 1,2-diaminoanthraquinone (DAQ) were used by Huang^[83] to create DADB. The DADB electrode has remarkable cycle lifetimes (more than 6000 cycles at 10 A g^{-1}) and excellent rate capability (71 mAh g^{-1} at 5 A g^{-1}) because of its extended conjugated structure and abundance of active sites. The electrochemical redox centers for Zn^{2+} storage are $\text{C}=\text{N}$ and $\text{C}=\text{O}$, as shown by ex-situ characterization experiments. However, the authors primarily analyzed the material from the electrochemical perspective and did not adequately explain the material's performance regarding its molecular structure. Therefore, more investigation is necessary to determine how these materials' molecular structure and electrochemical performance are related.

Most of the currently studied $-\text{NH}-$ bonded OEMs form Intra-HBs, and the number of bonds between the $-\text{NH}-$ and the active group atoms in intramolecular hydrogen bond rings may also affect the materials' properties. The theoretical capacity of IDAQ is 250 mAh g^{-1} , while the actual cyclic capacity of IDAQ combined with rGO is 150 mAh g^{-1} , and the uncombined cyclic capacity is 100 mAh g^{-1} , yielding the capacity utilization rate of 40% based on the uncombined capacity (Figure 6b). Similarly, the theoretical capacity of IDT is 242 mAh g^{-1} , with an actual cyclic capacity of 150 mAh g^{-1} when compounded with rGO, and the uncompounded cyclic capacity of 110 mAh g^{-1} , resulting in the capacity utilization rate of 45% based on the uncompounded capacity (Figure 6c). The theoretical capacity of DADB is 295 mAh g^{-1} , with the actual cyclic capacity of 134 mAh g^{-1} , and the capacity utilization rate of 45% (Figure 6d). From the above data, it is evident that the utilization rate of the active sites in these untreated materials containing $-\text{NH}-$ is 40–50%. This may be due to the formation of stable six-membered Intra-HBs by $-\text{NH}-$ occupying the active sites, resulting in insufficient utilization of the active groups, or the steric hindrance effect leading to difficulties in ion insertion. However, this is a hypothesis, and specific reasons need to be further investigated through experiments.

5. Amino ($-\text{NH}_2$) Hydrogen Bonds in Organic Electrode Materials

As potent hydrogen bond donors (HBDs), the $-\text{NH}_2$ group exhibits distinct characteristics. Unlike $-\text{OH}$ and $-\text{NH}-$, which can each donate only one H, $-\text{NH}_2$'s ability to donate two H significantly enhances its functionality. This dual proton-donating

capacity makes its role in hydrogen bonds particularly important within battery systems. Only in recent years have researchers increasingly focused on the impact of $-\text{NH}_2$ hydrogen bonds on battery performance, yielding notable results.

The investigation into the role of NH_2 hydrogen bonds is crucial for advancing the development of OEMs.

5.1. The Role of $-\text{NH}_2$ Hydrogen Bonds in Proton-Free Electrolytes

The presence of $-\text{NH}_2$ in material molecules can enhance their electrical conductivity. Additionally, the constructed hydrogen bond networks can improve the material's stability and accelerate ion transport. The usage of active sites is further encouraged by the creation of Inter-HBs. Pyrene-4,5,9,10-tetraone (PTO) is a carbonyl-rich compound with four $\text{C}=\text{O}$ functional groups that can serve as HBAs with a high theoretical capacity as the active monomer ($\text{Ctheo} = 408 \text{ mAh g}^{-1}$). Zheng et al.^[84] introduced amino groups ($-\text{NH}_2$) into PTO through elaborate molecular design to obtain 2,7-diamino-4,5,9,10-tetraone (PTO- NH_2) and proposed creating hydrogen bond networks by forming hydrogen bonds between molecules in order to prevent active compounds from becoming soluble. PTO- NH_2 features three types of hydrogen bonds – intermolecular N-H...O (2.20 \AA), intramolecular C-H...O (2.50 \AA), and intermolecular C-H...O (2.57 \AA) (Figure 7a). These bonds caused PTO- NH_2 to exhibit transverse 2D extension and longitudinal π -stack structures. The reversible evolution of hydrogen bonds was monitored by in-situ FTIR spectroscopy, which confirmed that the hydrogen bond networks maintain the intermediate state of the 2-electron reaction. DFT calculations show that the introduction of $-\text{NH}_2$ raised the lowest unoccupied molecular orbital (LUMO) and the highest occupied molecular orbital (HOMO) energy levels. However, the E_g (LUMO-HOMO gap) of PTO- NH_2 (2.46 eV) was less than that of PTO (3.49 eV). Consequently, the voltage gap between the PTO- NH_2 reduction peak and the platform was lower than that of PTO, resulting in higher conductivity for PTO- NH_2 . Due to its high conjugation and electronic conductivity, higher active site usage rates are attained by PTO- NH_2 (349 mAh g^{-1} , 95% $\text{Ctheo} = 367 \text{ mAh g}^{-1}$) compared to PTO (352 mAh g^{-1} , 86% $\text{Ctheo} = 408 \text{ mAh g}^{-1}$). Therefore, PTO- NH_2 , with its hydrogen bond networks structure, achieved superior rate performance (280 mAh g^{-1} at 1 A g^{-1}), and excellent cycle stability (83% capacity retention after 100 cycles).

After reasonable structural design, the $-\text{NH}_2$ group can form the networks of Intra-HBs and Inter-HBs. In 2019, Sieuw et al.^[85] applied 2,5-diamino-1,4-benzoquinone (DABQ) to LIBs and discovered that in organic electrolytes, it has extremely little solubility. In-situ XRD and ex-situ FTIR tests revealed that fully reversible chemical and structural changes occurred during the electrochemical cycling of DABQ, demonstrating the exceptional stability of its molecular crystals and the stability of its charge and discharge processes. The amount of salt present in the electrolytes influences the material's disintegration as well. Generally, high salt concentrations inhibited the dissolution of electrode materials, however, high salt concentrations promoted the dissolution of DABQ. The authors proposed that the solvent-salt molar ratio (MR) affects the solubility of DABQ to explain this phenomenon. When $\text{MR} < 4.25$, the solvent salt

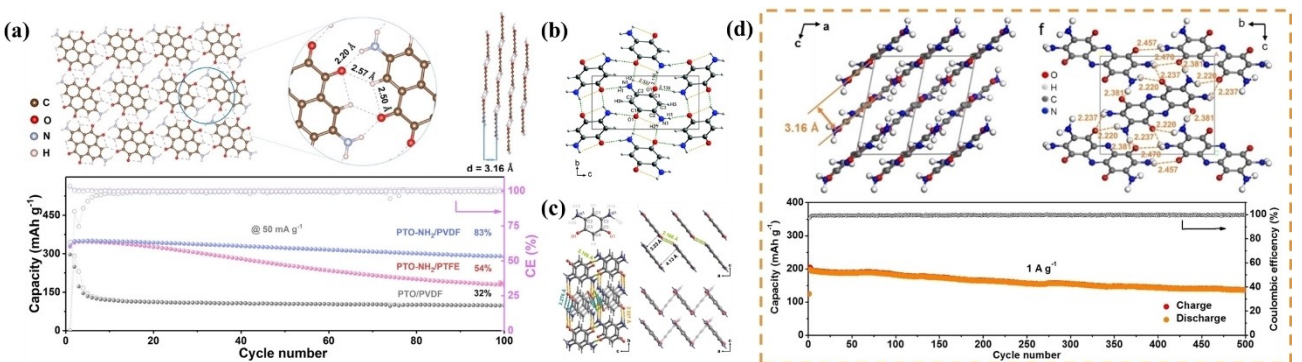


Figure 7. a) PTO-NH₂ hydrogen bond structure, and cyclic performance of Li||PTO-NH₂ batteries at 50 mA g⁻¹. Reproduced from Ref.^[84] with permission, Copyright (2022) Wiley-VCH. b) DABQ hydrogen bond structure. Reproduced from Ref.^[85] with permission. Copyright (2019) The Royal Society of Chemistry. c) 4,6 DA 1,3 BQ hydrogen bond structure. This figure has been published in CCS Chemistry [2022]. [Diradicals or Zwitterions: The Chemical States of m-Benzoquinone and Structural Variation after Storage of Li Ions] is available online at [10.31635/ccschem.021.202101333] d) The hydrogen bond structure of TAPT, and cyclic performance of TAPT||TAPT at 1 A g⁻¹. Reproduced from Ref.^[87] with permission, Copyright (2022) Wiley-VCH.

coordination environment was unsaturated, resulting in remaining free sites interacting with DABQ molecules and leading to DABQ dissolution. This theory may apply to other organic materials as well. Chemical modification of the $-\text{NH}_2$ groups weakened the strength of hydrogen bonds and was detrimental to the stability of the materials, as verified by other works conducted by the authors. They synthesized two derivatives of DABQ (N-methyl and N-ethyl derivatives), but these did not perform as well as DABQ in dissolution tests. This demonstrated that the hydrogen bonds effect of $-\text{NH}_2$ groups significantly influenced material properties. Combined with the calculated crystal structure of DABQ, it was shown that the hydrogen in the $-\text{NH}_2$ group forms both Intra-HBs and Inter-HBs, and the combined action of these bonds contributed to the intrinsic structural stability of DABQ (Figure 7b).

Research on the hydrogen bond interactions between OEMs and electrolytes is limited. It is generally believed that the electrolyte may compete with the hydrogen bonds within the molecule, thereby weakening them. However, the exact mechanism remains unclear and requires further exploration. Zhang et al.^[86] investigated the chemical structures of the small molecule m-benzoquinone 4,6-diamino-1,3-benzoquinone (4,6 DA 1,3 BQ), its solubility in various lithium salt electrolytes, and its structural transformation post-lithium storage (Figure 7c). Because zwitterions and hydrogen bonds were present, 4,6 DA 1,3 BQ showed a strong dependency on lithium salts and solvents. Their studies indicated that the type and concentration of salt significantly affect the solubility of 4,6 DA 1,3 BQ, primarily because of the competition between free lithium ions and Inter-HBs, leading to the weakening of hydrogen bonds. This finding was confirmed by UV-visible light spectra analysis, consistent with Sieuw's conclusions. Li et al.^[87] from the same research group studied the small molecule 2,3,7,8-tetraamino-phenazine-1,4,6,9-tetraone (TAPT) for use in symmetric all-organic batteries (SAOBs). TAPT exhibited exceptional thermal stability, with decomposition temperatures exceeding 200 °C. Under TEM, TAPT displayed the layered lamellar structure, indicating strong intermolecular interactions within the plane. DFT calculations revealed that hydrogen bonds formed

between the C=O and $-\text{NH}_2$ groups of adjacent molecules in the interlayer, and these abundant strong hydrogen bonds led to the material's layered accumulation and lamellar structure. As reversible redox-active sites, the C=O and C=N enabled TAPT to respectively transfer 4 and 2 electrons at about 2.5 V and 0.75 V (vs. Li⁺/Li) according to plentiful tests. This enabled TAPT to function as both the cathode and anode in SAOBs. Thanks to hydrogen bonds and π - π interactions, TAPT-assembled all-organic batteries achieved a capacity of up to 198 mAh g⁻¹ at 1 A g⁻¹ (Figure 7d), with an average operating voltage of about 2 V even after 500 cycles, and the energy density of approximately 147 Wh kg⁻¹.

5.2. The Role of $-\text{NH}_2$ Hydrogen Bonds In Proton-Containing Electrolytes

In electrolytes containing protons, the formation of $-\text{NH}_2$ hydrogen bond networks between molecules not only stabilizes the material but also facilitates proton migration. Consequently, H⁺ storage exhibits unique advantages compared to other carrier ions. In 2021, Lin et al.^[88] employed tetraamino-p-benzoquinone (TABQ) in AZIBs and highlighted that the hydrogen bond networks formed by C=O and $-\text{NH}_2$ groups on TABQ molecules provided low activation energy for charge transfer and proton diffusion by enabling proton conduction via the Grotthuss mechanism. With 0.1 A g⁻¹, the TABQ cathode electrode provided the high capacity (303 mAh g⁻¹) in AZIBs after 1000 stable cycles, it retained the capacity of 213 mAh g⁻¹, even at current densities as high as 5 A g⁻¹ (Figure 8a). The authors' other significant work investigated the dissolution problems of tetrahydroxy-p-benzoquinone (THBQ), tetraamino-p-benzoquinone (TABQ), and tetrachloroo-benzoquinone (o-TCBQ) in the 1 M ZnSO₄ electrolyte. They noted that THBQ and TABQ have higher solubilities than o-TCBQ due to their hydrophilic functional groups of $-\text{OH}$ or $-\text{NH}_2$. However, the highly symmetrical molecular structures and low dipole moment of these compounds resulted in relatively low solubility compared to BQ. The authors also explored proton storage in TABQ,

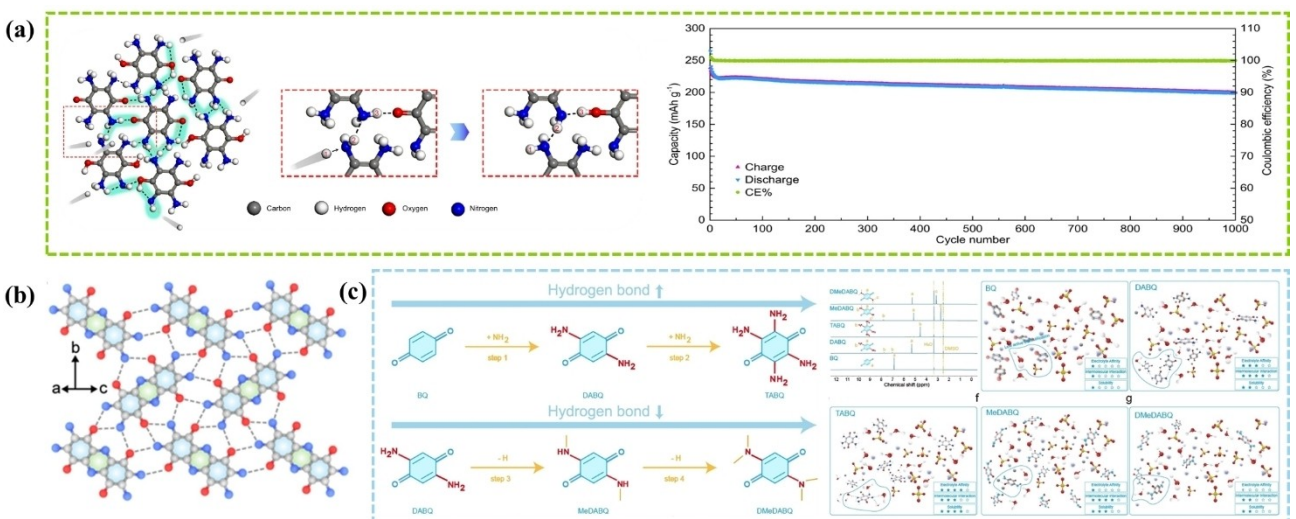


Figure 8. a) Schematic illustration for the proton conduction manner in the hydrogen bond networks in TABQ, and cyclic performance of $Zn \parallel TABQ$ at 5 A g^{-1} . Reproduced from Ref.^[88] with permission. Copyright (2021) Springer Nature. b) The hydrogen bond structure of BTABQ. Reproduced from Ref.^[90] with permission. Copyright (2023) Elsevier B.V. c) Design of hydrogen bond evolution model for AZIBs, and progressive and breakage model of the quinone-based hydrogen bond structures schematic diagrams of the BQ, DABQ, TABQ, MeDABQ, and DMeDABQ in AZIBs. Reproduced from Ref.^[91] with permission, Copyright (2024) Wiley-VCH.

attributing it to the presence of the TABQ hydrogen bond networks. Previous studies have shown that in neutral or weakly acidic electrolytes, C=O protonation on quinones was difficult and negligible due to low proton activity. However, the active protonation/deprotonation of the $-\text{NH}_2$ group gave TABQ the advantage in proton storage.

The electrochemical properties of 2,3,7,8-tetraamino-5,10-dihydrophenazine-1,4,6,9-tetraone (TDT), polymerized from two molecules of tetraamino-p-benzoquinone (TABQ) in an aqueous electrolyte, were investigated. In 2023, Lin et al.^[89] synthesized the piperazine-linked quinone TDT, for AZIBs using the condensation reaction between two TABQ molecules. SEM images revealed that TABQ had the short rod-like shape, and TGA indicated a significant weight loss above 300°C , primarily due to Inter-HBs introduced by $-\text{NH}_2$ groups. According to theoretical studies, there was extended conjugation between π electrons on nitrogen and π electrons on the quinone ring, which caused electron delocalization throughout the molecule. The cationic radicals were found to develop on the nitrogen of the piperazine ring, and conjugated structures stabilized free radicals, hence increasing electrical conductivity, according to electron paramagnetic resonance (EPR) examination. In AZIBs, the TDT cathode electrode containing 10% carbon exhibited a high capacity of 369 mAh g^{-1} at 0.2 A g^{-1} and maintained a capacity of 182 mAh g^{-1} at 10 A g^{-1} . For 3000 cycles of steady cycling, in-situ UV-VIS analysis verified that TDT was insoluble in all charge/discharge states. In the same year, Chen et al.^[90] synthesized bis-tetraaminobenzoquinone (BTABQ) and its polymer analog poly(bis-tetraaminobenzoquinone) (pBTABQ). Single-crystal data of BTABQ were obtained, demonstrating its use as the organic material for electrochemical energy storage. BTABQ and pBTABQ contained a high density of redox-active C=O groups, $-\text{NH}-$ groups, and extended conjugated aromatic scaffolds. These compounds were insoluble in both organic and

aqueous media due to hydrogen bonds and π - π interactions between the donors and acceptors (Figure 8). BTABQ and pBTABQ exhibit high charge storage capacity at a high charge-discharge rate, which may be attributed to the fast pseudo-capacitive insertion process. The extended electron delocalization and rapid ion transport enabled charge storage and transport throughout the electrode bulk, even under practical mass loads. Compared to small organic molecules that exhibit hydrogen bonds but lack extended conjugation, and molecules with extensive conjugation but lack hydrogen bonds, fused aromatic frameworks with extended conjugation, hydrogen bonds, and π - π stacking were crucial for pseudo-capacitive charge storage in organic materials. Additionally, the pH of the electrolyte, hydrogen bonds, and ion size significantly affected the electrochemical properties of BTABQ and pBTABQ. In acidic electrolytes, protons were transported through the Grotthuss mechanism in pBTABQ's extensive hydrogen bond networks, enhancing the stability of BTABQ during reactions.

The quantity of $-\text{NH}_2$ hydrogen bonds has a considerable impact on the characteristics of electrode materials. Guo et al.^[91] designed five materials with varying numbers of hydrogen bonds – 2,5-bis(dimethylamino)cyclohexa-2,5-diene-1,4-dione (DMeDABQ), 2,5-bis(methylamino)cyclohexa-2,5-diene-1,4-dione (MeDABQ), 2,3,5,6-tetraaminocyclohexa-2,5-diene-1,4-dione (TABQ), 2,5-diaminocyclohexa-2,5-diene-1,4-dione (DABQ), and benzoquinone (BQ) (Figure 8c), and investigated their electrochemical properties in AZIBs. MeDABQ disrupted the Inter-HBs, resulting in poor thermal stability. However, the presence of the -Me group activated the nitrogen at the adjacent site, making it an active center for energy storage, thereby slightly increasing capacity. DMeDABQ exhibited poor capacity and reversibility because all the hydrogen atoms in the $-\text{NH}_2$ group were occupied. Variable temperature FTIR tests showed that high temperatures weaken hydrogen bond interactions while in-

creasing the number of hydrogen bonds under vacuum conditions enhances intermolecular interactions. However, in the aqueous electrolyte, materials with vast HBDs form numerous hydrogen bonds with the electrolyte, weakening the intermolecular hydrogen bond interactions and enhancing material dissolution. This results in poor cycle stability of the batteries. Optimal performance in the battery is achieved with the right number of hydrogen bonds in the material. The study found that DABQ with a reasonable number of HBDs, achieved the best performance. At $5\text{ A}\text{g}^{-1}$, a high capacity of 376.3 mAh g^{-1} (97% active site utilization) was achieved, and after 1500 cycles 100% capacity was retained. DABQ offered a reversible capacity of more than 193.3 mAh g^{-1} even with the increased load mass of 66.2 mg cm^{-2} .

6. Summary and Outlook

Organic electrode materials (OEMs) hold significant development potential in the field of batteries, serving as a powerful supplement to resource-limited inorganic electrode materials. This review summarizes the roles of hydroxyl ($-\text{OH}$), imino ($-\text{NH}-$), and amino ($-\text{NH}_2$) hydrogen bonds in the electrochemical redox processes of OEMs. When reasonable distances exist between the hydrogen bond acceptors (HBAs) and hydrogen bond donors (HBDs), the hydrogen bonds are generally preferentially formed within the molecule. The presence of hydrogen bond networks can promote ion transfer, increase the bulk density of the material, enhance electrical conductivity, improve structural stability, and inhibit material dissolution during cycling.

Below is a summary of the three main roles that various hydrogen bond donors play in OEMs: (1) The reversible conversion of $-\text{OH}$ and C=O groups facilitates adjustments in the electrochemical process. Although hydrogen bond networks may occupy active sites to some extent, the presence of the $-\text{OH}$ groups can increase the activity of the active group, thereby enhancing the utilization rate of the active sites. Consequently, most organic molecules containing $-\text{OH}$ groups exhibit stable cyclic reversibility and high-capacity performance. (2) $-\text{NH}-$ groups can undergo reversible transformation with the C=N groups under certain conditions. However, unlike OEMs containing hydroxyl groups, the properties of materials containing $-\text{NH}-$ may more depend on the type of hydrogen bonds they form. The strong hydrogen bonds formed between $-\text{NH}-$ and the active site may be difficult to break, resulting in low material dissolution during cycling but relatively poor capacity performance. (3) $-\text{NH}_2$ groups can provide two H, offering the unique advantage in constructing intermolecular and intramolecular multiple hydrogen bond networks. This capability facilitates high conductivity, high ion migration, and high stability in energy storage materials. In recent years, the applications of $-\text{NH}_2$ compounds in batteries have expanded, mainly because the syntheses of containing $-\text{NH}_2$ compounds are relatively complex compared to those containing $-\text{OH}$ or $-\text{NH}-$ groups. Nonetheless, their superior functionality and

potential in proton energy storage make them highly valuable for research as energy storage materials.

Hydrogen bonds play crucial roles in OEMs. Introducing the appropriate number of HBDs can enhance the structural stability of the reaction process and improve the utilization of active sites, thereby enhancing the overall performance of organic batteries. The thoughtful design of hydrogen bonds in these materials can lead to the optimization of their properties. Research on hydrogen bond science is an effective approach to addressing issues such as low capacity, low conductivity, and the dissolution of organic materials. However, there are few studies on the hydrogen bonds between organic materials and electrolytes or other components, and exploring hydrogen bonds between different parts of the batteries is a promising future research direction. Currently, the researches on hydrogen bonds are limited to traditional characterization methods, such as Infrared spectroscopy, Raman spectroscopy, and Nuclear magnetic resonance. Future research should incorporate new characterization methods in the field of batteries. Cultivating single crystals and analyzing their data are effective methods for determining the hydrogen bond structures of materials, therefore, attention should also be given to the cultivation of single crystals of OEMs.

Studying OEMs from the perspective of hydrogen bonds is undeniably one of the most promising directions for developing the next generation of organic batteries. However, it is important not to overstate the impact of hydrogen bonds. Only by conducting objective research and analysis on hydrogen bond science in the appropriate context can their potential be fully realized in the battery field. We hold great expectations for the future of OEMs.

Acknowledgements

This work was financially supported by the National Natural Science Foundation of China (No. 21875206), the Subsidy for Hebei Key Laboratory of Applied Chemistry after Operation Performance (No. 22567616H), The Performance Subsidy Fund for Key Laboratory of Dielectric and Electrolyte Functional Material Hebei Province (No. 22567627H), P.R. China. Q.Z. thanks to the support from City University of Hong Kong (9380117, 7005620, 7020040, and 7020089) and Hong Kong Institute for Advanced Study, City University of Hong Kong.

Conflict of Interests

The authors declare no conflict of interest.

Keywords: Batteries • Hydrogen bonds • Intermolecular interaction • Intramolecular interaction • Organic electrode materials

[1] D. L. Williams, J. J. Byrne, J. S. Driscoll, *J. Electrochem. Soc.* **1969**, *116*, 2.

- [2] H. Alt, H. Binder, A. Köhling, G. Sandstede, *Electrochim. Acta* **1972**, *17*, 873–887.
- [3] T. Ohzuku, H. Wakamatsu, Z. Takehara, S. Yoshizawa, *Electrochim. Acta* **1979**, *24*, 723–726.
- [4] T. Kobayashi, H. Yoneyama, H. Tamura, *J. Electroanal. Chem.* **1984**, *177*, 281–291.
- [5] W. Huang, Z. Zhu, L. Wang, S. Wang, H. Li, Z. Tao, J. Shi, L. Guan, J. Chen, *Angew. Chem. Int. Ed.* **2013**, *52*, 9162–9166.
- [6] T. Sun, Q. Sun, Y. Yu, X. Zhang, *escience* **2021**, *1*, 186–193..
- [7] Y. Tong, J. Wang, Z. Sun, W. Huang, *ACS Appl. Mater. Interfaces* **2023**, *15*, 14274–14281.
- [8] Z. Tie, L. Liu, S. Deng, D. Zhao, Z. Niu, *Angew. Chem. Int. Ed.* **2020**, *59*, 4920–4924.
- [9] K.-K. Liu, Z. Meng, Y. Fang, H.-L. Jiang, *eScience* **2023**, *3*, 100133.
- [10] W. M. Latimer, W. H. Rodebush, *J. Am. Chem. Soc.* **1920**, *42*, 1419–1433.
- [11] M. L. Huggins, *J. Phys. Chem.* **1936**, *40*, 723–731.
- [12] E. Arunan, G. R. Desiraju, R. A. Klein, J. Sadlej, S. Scheiner, I. Alkorta, D. C. Clary, R. H. Crabtree, J. J. Dannenberg, P. Hobza, H. G. Kjaergaard, A. C. Legon, B. Mennucci, D. J. Nesbitt, *Pure Appl. Chem.* **2011**, *83*, 1619–1636.
- [13] J. Zhang, P. Chen, B. Yuan, W. Ji, Z. Cheng, X. Qiu, *Science* **2013**, *342*, 611–614.
- [14] L. J. Karas, C. H. Wu, R. Das, J. I. C. Wu, *WIREs Comput. Mol. Sci.* **2020**, *10*, e1477.
- [15] a) D. J. Sutor, *Nature* **1962**, *195*, 68–69; b) G. R. Desiraju, *Acc. Chem. Res.* **1996**, *29*, 441–449.
- [16] a) M. Harigai, M. Kataoka, Y. Imamoto, *J. Am. Chem. Soc.* **2006**, *128*, 10646–10647; b) X. Zhang, H. Dai, H. Yan, W. Zou, D. Cremer, *J. Am. Chem. Soc.* **2016**, *138*, 4334–4337.
- [17] a) R. H. Crabtree, P. E. M. Siegbahn, O. Eisenstein, A. L. Rheingold, T. F. Koetzle, *Acc. Chem. Res.* **1996**, *29*, 348–354; b) K. Verma, K. S. Viswanathan, *Phys. Chem. Chem. Phys.* **2017**, *19*, 19067–19074.
- [18] M. S. Taylor, E. N. Jacobsen, *Angew. Chem. Int. Ed.* **2006**, *45*, 1520–1543.
- [19] H. Zhang, D. Xu, L. Wang, Z. Ye, B. Chen, L. Pei, Z. Wang, Z. Cao, J. Shen, M. Ye, *Small* **2021**, *17*, 2100902.
- [20] M. R. Tuttle, S. T. Davis, S. Zhang, *ACS Energy Lett.* **2021**, *6*, 643–649.
- [21] R. Gao, Q. Zhang, Y. Zhao, Z. Han, C. Sun, J. Sheng, X. Zhong, B. Chen, C. Li, S. Ni, Z. Piao, B. Li, G. Zhou, *Adv. Funct. Mater.* **2022**, *32*, 2110313.
- [22] Z. Cui, Z. Jia, D. Ruan, Q. Nian, J. Fan, S. Chen, Z. He, D. Wang, J. Jiang, J. Ma, X. Ou, S. Jiao, Q. Wang, X. Ren, *Nat. Commun.* **2024**, *15*, 2033.
- [23] J. Zhang, P. Chen, B. Yuan, W. Ji, Z. Cheng, X. Qiu, *Science* **2013**, *342*, 611–614.
- [24] Y. Deng, Q. Zhang, D.-H. Qu, *ACS Materials Lett.* **2023**, *5*, 480–490.
- [25] L. Pauling, R. B. Corey, *Nature* **1953**, *171*, 59–61.
- [26] a) T. Sun, Q. Nian, X. Ren, Z. Tao, *Joule* **2023**, *7*, 2700–2731; b) D. Duan, X. Cai, C. Ma, Z. Lin, Y. Wang, J. Nai, T. Liu, J. Luo, Y. Liu, X. Tao, *Sci. China Chem.* **2023**, *66*, 1905–1923.
- [27] T. Van Duong, G. Reekmans, A. Venkatesham, A. Van Aerschot, P. Adriaensens, J. Van Humbeeck, G. Van den Mooter, *Mol. Pharmaceutics* **2017**, *14*, 1726–1741.
- [28] S. P. Verevkin, D. H. Zaitsau, K. V. Zherikova, *J. Mol. Liq.* **2023**, *382*, 121938.
- [29] K. M. Harmon, S. H. Gill, P. G. Rasmussen, G. L. Hardgrove Jr, *J. Mol. Struct.* **1999**, *478*, 145–154.
- [30] Q. Zhao, W. Huang, Z. Luo, L. Liu, Y. Lu, Y. Li, L. Li, J. Hu, H. Ma, J. Chen, *Sci. Adv.* **2018**, *4*, eaao1761.
- [31] Z. Wang, Y. Zhang, P. Zhang, D. Yan, J. Liu, Y. Chen, Q. Liu, P. Cheng, M. J. Zaworotko, Z. Zhang, *escience* **2022**, *2*, 311–318..
- [32] J. Wang, Y. Tong, W. Huang, Q. Zhang, *Batteries & Supercaps* **2023**, *6*, e202200413.
- [33] Y. Shi, Y. Lin, F. Kang, N. Aratani, W. Huang, Q. Zhang, *ACS Appl. Mater. Interfaces* **2022**, *15*, 1227–1233.
- [34] Y. Chen, Y. Gao, C. Zhang, J. Zou, K. Fan, Z. Li, G. Zhang, C. Wang, *Scientia Sinica Chimica* **2022**, *52*, 1883–1895.
- [35] Z. Song, Y. Qian, X. Liu, T. Zhang, Y. Zhu, H. Yu, M. Otani, H. Zhou, *Energy Environ. Sci.* **2014**, *7*, 4077–4086.
- [36] M. Li, X. Wang, J. Meng, C. Zuo, B. Wu, C. Li, W. Sun, L. Mai, *Adv. Mater.* **2024**, *36*, 2308628.
- [37] Y. Chen, J. Li, Q. Zhu, K. Fan, Y. Cao, G. Zhang, C. Zhang, Y. Gao, J. Zou, T. Zhai, C. Wang, *Angew. Chem. Int. Ed.* **2022**, *61*, e202116289.
- [38] T. A. Hubbard, A. J. Brown, I. A. W. Bell, S. L. Cockcroft, *J. Am. Chem. Soc.* **2016**, *138*, 15114–15117.
- [39] F. A. Martins, M. P. Freitas, *ACS Omega* **2018**, *3*, 10250–10254.
- [40] P. Froimowicz, K. Zhang, H. Ishida, *Chem. Eur. J.* **2016**, *22*, 2691–2707.
- [41] M. Saccone, M. Pfletscher, S. Kather, C. Wölper, C. Daniliuc, M. Mezger, M. Giese, *J. Mater. Chem. C* **2019**, *7*, 8643–8648.
- [42] H. Yuan, S. Feng, K. Wen, X. Guo, J. Zhang, *Spectrochim. Acta Part A* **2018**, *191*, 421–426.
- [43] a) M. Martínez-Cifuentes, W. Cardona, C. Saitz, B. Weiss-López, R. Araya-Maturana, *Molecules* **2017**, *22*, 593; b) F. Ji, Z. Wu, M. Wang, Y. Guo, C. Wang, S. Wang, G. Zhao, *J. Lumin.* **2022**, *248*, 118914.
- [44] Q. Zhao, Z. Zhu, J. Chen, *Adv. Mater.* **2017**, *29*, 1607007.
- [45] Y. Lu, Y. Cai, Q. Zhang, J. Chen, *Adv. Mater.* **2022**, *34*, 2104150.
- [46] Z. Luo, S. Zheng, S. Zhao, X. Jiao, Z. Gong, F. Cai, Y. Duan, F. Li, Z. Yuan, *J. Mater. Chem. A* **2021**, *9*, 6131–6138.
- [47] a) H. Peng, J. Xiao, Z. Wu, L. Zhang, Y. Geng, W. Xin, J. Li, Z. Yan, K. Zhang, Z. Zhu, *CCS* **2023**, *5*, 1789–1801; b) T. Sun, W. Zhang, Q. Nian, Z. Tao, *Nano-Micro Lett.* **2023**, *15*, 36.
- [48] Y. Song, Q. Qin, L. Jing, M. Li, H. Zhao, J. Cui, Y. Zhang, *Composites Part B* **2023**, *252*, 110517.
- [49] Y. Hanyu, Y. Ganbe, I. Honma, *J. Power Sources* **2013**, *221*, 186–190.
- [50] K. Kon, K. Uchida, K. Fuku, S. Yamanaka, B. Wu, D. Yamazui, H. Iguchi, H. Kobayashi, Y. Gambe, I. Honma, S. Takaishi, *ACS Appl. Mater. Interfaces* **2021**, *13*, 38188–38193.
- [51] T. Cai, Z. Hu, Y. Gao, G. Li, Z. Song, *Energy Storage Mater.* **2022**, *50*, 426–434.
- [52] Y. Wu, J. Shen, Z. Sun, Y. Yang, F. Li, S. Ji, M. Zhu, J. Liu, *Angew. Chem. Int. Ed.* **2022**, *62*, e202215864.
- [53] X. Gao, Y. Wang, L. T. Menezes, Z. Huang, H. Kleinke, Y. Li, *Adv. Funct. Mater.* **2024**, *34*, 2315669.
- [54] S. Zheng, S. Yu, Z. Ullah, L. Liu, L. Chen, H. Sun, M. Chen, L. Liu, Q. Li, *J. Mater. Chem. A* **2024**, *12*, 3967–3976.
- [55] H. J. Kim, Y. Kim, J. Shim, K. H. Jung, M. S. Jung, H. Kim, J.-C. Lee, K. T. Lee, *ACS Appl. Mater. Interfaces* **2018**, *10*, 3479–3486.
- [56] Q. Jiang, P. Xiong, J. Liu, Z. Xie, Q. Wang, X. Q. Yang, E. Hu, Y. Cao, J. Sun, Y. Xu, L. Chen, *Angew. Chem. Int. Ed.* **2020**, *59*, 5273–5277.
- [57] J. Geng, Y. Ni, Z. Zhu, Q. Wu, S. Gao, W. Hua, S. Indris, J. Chen, F. Li, J. Am. Chem. Soc. **2023**, *145*, 1564–1571.
- [58] K. Li, J. Yu, Z. Si, B. Gao, H. Wang, Y. Wang, *Chem. Eng. J.* **2022**, *450*, 138052.
- [59] C. Liang, X. Cai, J. Lin, Y. Chen, Y. Xie, Y. Liu, *ChemPlusChem* **2024**, *89*, e202300620.
- [60] D. Pakulski, V. Montes-García, A. Gorczyński, W. Czepa, T. Chudziak, M. Bielejewski, A. Musiał, I. Pérez-Juste, P. Samorì, A. Ciesielski, *J. Mater. Chem. A* **2024**, *12*, 440–450.
- [61] J. Huang, S. Li, E. Y. Kim, L. Cheng, G.-L. Xu, K. Amine, C. Wang, C. Luo, *Small Structures* **2023**, *4*, 2300211.
- [62] J. Lee, M. J. Park, *Adv. Energy Mater.* **2017**, *7*, 1602279.
- [63] A. Slesarenko, I. K. Yakuschenko, V. Ramezankhani, V. Sivasankaran, O. Romanyuk, A. V. Mumyatov, I. Zhidkov, S. Tsarev, E. Z. Kurmaev, A. F. Shestakov, O. V. Yarmolenko, K. J. Stevenson, P. A. Troshin, *J. Power Sources* **2019**, *435*, 226724.
- [64] M. Miroshnikov, K. Kato, G. Babu, N. Kumar, K. Mahankali, E. Hohenstein, H. Wang, S. Satapathy, K. P. Divya, H. Asare, L. M. R. Arava, P. M. Ajayan, G. John, *ACS Appl. Energ. Mater.* **2019**, *2*, 8596–8604.
- [65] Z. Hu, X. Zhao, Z. Li, S. Li, P. Sun, G. Wang, Q. Zhang, J. Liu, L. Zhang, *Adv. Mater.* **2021**, *33*, 2104039.
- [66] J. Yu, J. Li, Z. Y. Leong, D.-S. Li, J. Lu, Q. Wang, H. Y. Yang, *Mater. Today Energy* **2021**, *22*, 100872.
- [67] T. Sun, Z.-J. Li, Y.-F. Zhi, Y.-J. Huang, H. J. Fan, Q. Zhang, *Adv. Funct. Mater.* **2021**, *31*, 2010049.
- [68] Q. Sun, T. Sun, J. Du, Z. Xie, D. Yang, G. Huang, H. Xie, X. Zhang, *Angew. Chem. Int. Ed.* **2023**, *62*, e202307365.
- [69] T. Lap, N. Goujon, D. Mantione, F. Ruipérez, D. Mecerreyres, *ACS Appl. Polym. Mater.* **2023**, *5*, 9128–9137.
- [70] H. Cui, D. Zhang, Z. Wu, J. Zhu, P. Li, C. Li, Y. Hou, R. Zhang, X. Wang, X. Jin, S. Bai, C. Zhi, *Energy Environ. Sci.* **2024**, *17*, 114–122.
- [71] G. Zhao, X. Yan, Y. Dai, J. Xiong, Q. Zhao, X. Wang, H. Yu, J. Gao, N. Zhang, M. Hu, J. Yang, *Small* **2024**, *20*, 2306071.
- [72] Z. S. Safi, S. J. Al Hasanat, N. A. Wazzan, *J. Theor. Comput. Chem.* **2018**, *17*, 1850004.
- [73] T. W. Hiltermann, S. Sarkar, V. Thangadurai, T. C. Sutherland, *ACS Appl. Mater. Interfaces* **2024**, *16*, 8580–8588.
- [74] T. Shi, G. Li, Y. Han, Y. Gao, F. Wang, Z. Hu, T. Cai, J. Chu, Z. Song, *Energy Storage Mater.* **2022**, *50*, 265–273.
- [75] H. Zhang, R. Zhang, F. Ding, C. Shi, N. Zhao, *Energy Storage Mater.* **2022**, *51*, 172–180.
- [76] J. Xiong, X. Yan, H. Yu, C. Wu, G. Zhao, J. Zhang, Y. Dai, X. Wang, J. Gao, X. Pu, M. Hu, J. Liu, J. Yang, *J. Mater. Chem. A* **2023**, *11*, 8048–8056.
- [77] W. Zhang, T. Sun, W. Hao, M. Cheng, Z. Zha, M. Shi, Z. Tao, *Energy Storage Mater.* **2024**, *70*, 103561.

- [78] X. Geng, Y. Jiang, H. Ma, H. Zhang, J. Liu, Z. Zhang, C. Peng, J. Zhang, Q. Zhao, N. Zhu, *ACS Appl. Mater. Interfaces* **2022**, *14*, 49746–49754.
- [79] T. Sun, J. Pan, W. Zhang, X. Jiang, M. Cheng, Z. Zha, H. J. Fan, Z. Tao, *Nano-Micro Lett.* **2024**, *16*, 46.
- [80] J. Kumankuma-Sarpong, S. Tang, W. Guo, Y. Fu, *ACS Appl. Mater. Interfaces* **2021**, *13*, 4084–4092.
- [81] X. Geng, H. Ma, F. Lv, K. Yang, J. Ma, Y. Jiang, Q. Liu, D. Chen, Y. Jiang, N. Zhu, *Chem. Eng. J.* **2022**, *446*, 137289.
- [82] C. Peng, F. Wang, Q. Chen, X. Yan, C. Wu, J. Zhang, W. Tang, L. Chen, Y. Wang, J. Mao, S. Dou, Z. Guo, *Adv. Funct. Mater.* **2024**, *34*, 2401001.
- [83] L. Huang, J. Li, J. Wang, H. Lv, Y. Liu, B. Peng, L. Chen, W. Guo, G. Wang, T. Gu, *ACS Appl. Energ. Mater.* **2022**, *5*, 15780–15787.
- [84] S. Zheng, D. Shi, T. Sun, L. Zhang, W. Zhang, Y. Li, Z. Guo, Z. Tao, J. Chen, *Angew. Chem. Int. Ed.* **2022**, *62*, e202217710.
- [85] L. Sieuw, A. Jouhara, É. Quarez, C. Auger, J.-F. Gohy, P. Poizot, A. Vlad, *Chem. Sci.* **2019**, *10*, 418–426.
- [86] C. Zhang, Y. Zhang, K. Fan, Q. Zou, Y. Chen, Y. Wu, S. Bao, L. Zheng, J. Ma, C. Wang, *CCS* **2022**, *4*, 2768–2781.
- [87] Z. Li, Q. Jia, Y. Chen, K. Fan, C. Zhang, G. Zhang, M. Xu, M. Mao, J. Ma, W. Hu, C. Wang, *Angew. Chem. Int. Ed.* **2022**, *61*, e202207221.
- [88] Z. Lin, H.-Y. Shi, L. Lin, X. Yang, W. Wu, X. Sun, *Nat. Commun.* **2021**, *12*, 4424.
- [89] L. Lin, Z. Lin, J. Zhu, K. Wang, W. Wu, T. Qiu, X. Sun, *Energy Environ. Sci.* **2023**, *16*, 89–96.
- [90] T. Chen, H. Banda, L. Yang, J. Li, Y. Zhang, R. Parenti, M. Dincă, *Joule* **2023**, *7*, 986–1002.
- [91] J. Guo, J. Y. Du, W. Q. Liu, G. Huang, X. B. Zhang, *Angew. Chem. Int. Ed.* **2024**, *63*, e202406465.

Manuscript received: June 30, 2024

Revised manuscript received: July 26, 2024

Accepted manuscript online: August 15, 2024

Version of record online: October 17, 2024